Article:
Hassan, MM and Carr, CM (2018) A critical review on recent advancements of the removal of reactive dyes from dyehouse effluent by ion-exchange adsorbents. Chemosphere, 209. pp. 201-219. ISSN: 0045-6535

https://doi.org/10.1016/j.chemosphere.2018.06.043

A Critical Review on Recent Advancements of the Removal of Reactive Dyes from Dyehouse Effluent by Ion-exchange Adsorbents

Mohammad M. Hassan[1],* Christopher M. Carr[2]

[1] *Food & Bio-based Products Group, AgResearch Limited, Private Bag 4749, Christchurch 8140, New Zealand.*

[2] *School of Design, University of Leeds, Leeds LS2 5JQ, United Kingdom.*

Abstract

The effluent discharged by the textile dyehouses has a seriously detrimental effect on the aquatic environment. Some dyestuffs produce toxic decomposition products and the metal complex dyes release toxic heavy metals to watercourses. Of the dyes used in the textile industry, effluents containing reactive dyes are the most difficult to treat because of their high water-solubility and poor absorption into the fibers. A range of treatments has been investigated for the decolorization of textile effluent and the adsorption seems to be one of the cheapest, effective and convenient treatments. In this review, the adsorbents investigated in the last decade for the treatment of textile effluent containing reactive dyes including

* Corresponding author. Tel.: +64-3-321-8755, fax: +64-3-321-8811
E-mail address: mahbubul.hassan@agresearch.co.nz

modified clays, biomasses, chitin and its derivatives, and magnetic ion-exchanging particles have been critically reviewed and their reactive dye binding capacities have been compiled and compared. Moreover, the dye binding mechanism, dye sorption isotherm models and also the merits/demerits of various adsorbents are discussed. This review also includes the current challenges and the future directions for the development of adsorbents that meet these challenges. The adsorption capacities of adsorbents depend on various factors, such as the chemical structures of dyes, the ionic property, surface area, porosity of the adsorbents, and the operating conditions. It is evident from the literature survey that decolorization by the adsorption shows great promise for the removal of color from dyehouse effluent. If biomasses want to compete with the established ion-exchange resins and activated carbon, their dye binding capacity will need to be substantially improved.

Keywords: Decolorization, dyehouse effluent, reactive dyes, adsorption, ion-exchange, magnetic

1. **Introduction**

Textile industries, more specifically chemical processing textile industries, are at a crossroad because of the stringent guidelines and consent limits set by environmental agencies in various developed and developing countries for discharging effluent containing dyes and chemicals to watercourses. Textile dyeing and printing industries are under scrutiny because they discharge colored effluents to watercourses that quite easily draw the attention of general public.

A range of classes of dyes is used in textile industry including disperse, reactive, acid, basic, direct, azoic, sulfur, and direct dyes. Of them, vat, azoic, sulfur, and disperse dyes are insoluble in water and therefore easy to separate them from the effluent. On the other hand, reactive, direct, basic and acid dyes are highly soluble in water and therefore it is difficult to remove them from effluent by separation processes. All of these water-soluble dyes are anionic except the basic class of dyes, which is cationic. Table 1 and Fig. S1 (Supplementary Content) show dyestuff production data of India from 2012–2016 [Annual Report 2016–17] and China of 2016 [Ram, 2017] respectively that give an impression about the current scenario of global dyestuff production. These two countries are the largest dyestuff manufacturer in the world behind. It can be seen that reactive dyes are the second largest dye classes, which is mainly used for the dyeing of cellulosic fibers, and also a small percentage of silk and wool fibers. The reactive dyes left in the effluent cannot be reused as they become non-reactive due to hydrolysis. Because of their low adsorption and fixation, the reactive dye effluent is highly concentrated and difficult to treat by primary or secondary treatments. Therefore, the treatment of dyehouse effluent containing the reactive dyes is the most difficult to treat by conventional coagulation processes and the dyes are not biodegradable. Fig. 1 shows the chemical structure of several commonly investigated reactive dyes [Karcher et al., 2002].

The color is the main factor for which textile dyehouse effluent needs treatment as the deep color of the effluent impairs the penetration of light through water affecting the photosynthesis reactions to produce oxygen in water by underwater plants and thereby affecting the viability of aquatic animals and plants [Lambert and Davy, 2011]. Some dyes are not biodegradable or have very low biodegradability. Dyes and auxiliaries increase the total dissolved solids content, total suspended solids content and also the chemical oxygen demand and biological oxygen demand of the effluent that negatively affects the aquatic

ecological system. Some reactive dyes are metal complexed with copper, chromium, and nickel. When these dyes degrade, they release toxic heavy metals into the environment that can end up in the food chain.

Several reviews have been published in the area of removal of dyes from effluent by adsorption [Yagub et al., 2014; Bharathi et al., 2013; Pearce et al., 2003], but they have targeted either a specific dye or a specific type of adsorbent. Some of these reviews are quite old and, in the meantime, many high performing adsorbents have been developed. None of the previous reviews specifically addressed the treatment of effluent containing reactive dyes (the most problematic of the dye classes used in textile industry) and compared the dye-binding capacities of various ion-exchange type adsorbents. In this review, ion-exchange type modified clays, cellulosic and microbial biomasses, chitosan and its derivatives, and magnetic particles with their reactive dye binding capacities, have been compiled, presented and compared.

2. Types of ion-exchange adsorbents

The ion-exchange adsorbents imply by name that they bind pollutants of opposite charge. As the reactive dyes are anionic, only anion-exchanging adsorbents have been covered in this review. A range of adsorbents, such as clay [Aguiar et al., 2013], ion-exchange resins [Karcher et al., 2002], lignocellulosic biomasses [Honorio et al., 2016], and microbial biomasses [Aytar et al., 2016], have been investigated for the removal of color from reactive dye effluent.

2.1. Clay type adsorbents and their dye binding performance

2.1.1. Clay adsorbents

The type of clays, especially those that are rich in iron and aluminum, can be used for the removal of reactive dyes from the effluent. Some of the clay-type adsorbents are synthetically made (e.g. layered double hydroxides), while others are waste products of industrial processing (e.g. red mud). Both calcined and non-calcined types of clays have been investigated for the removal of reactive dyes but the calcined clays are preferred over non-calcined clays due to their higher surface area and also they show better dye binding capacity [Aguiar et al., 2013; Asouhidou et al., 2012]. The clay-like materials investigated for the removal of reactive dyes include nano-hydroxyapatite [Kyzas et al., 2013], layered double hydroxides (LDH) [Sumari et al., 2016; Aguiar et al., 2013; Asouhidou et al., 2012], $Mg(OH)_2$-modified-kaolin [Amin et al., 2015], and also the sea-water neutralized and calcined red mud [de Jesus et al., 2015; de Souza et al., 2013; Wang et al., 2009]. The laccase-modified fumed silica [Kalkan et al., 2014], nano-alumina [Nadafi et al., 2014], zinc and magnesium oxide nanoparticles [Khoshhesab et al., 2015; Venkatesha et al., 2012], kaolinite and smectite [Errais et al., 2012], $Mg(OH)_2$-coated bentonite [Chinoune et al., 2016], silylated palygorskite [Xue et al., 2010], and synthetic talc [Rahman et al., 2013] also can be included in this list of clay-like materials.

2.1.2. Reactive dye binding capacity of clay-like adsorbents and dye binding mechanisms

The dye binding capacities, the pH of maximum adsorption, and operating conditions of removal of reactive dyes by clay-like adsorbents are shown in Table S1 (Supplementary Content). Raw kaolinite, Fouchana clay, and synthetic talc showed quite meager reactive dye

binding capacity [Errais et al., 2012, Rahman et al., 2013]. On the other hand, laccase modified fumed silica [Kalkan et al., 2014], seawater-neutralized red mud calcined at 500 °C [de Jesus et al., 2015], and calcined Mg/Al LDH [Sumari et al., 2016] showed quite good dye binding capacity. Of the clays investigated, non-calcined Mg/Al LDH showed the highest reactive dye binding capacity for the removal of C.I. Reactive Blue 4 (328.9 mg g^{-1}) [Aguiar et al., 2013].

2.1.3. Reactive dye binding mechanisms

Fig. 2 shows the chemical structure of a few clay-type adsorbents and their reactive dye binding mechanisms. Aluminum and iron are tri and di or trivalent metals respectively with positive charges and therefore aluminum and iron-rich clays can electrostatically bind anionic reactive dyes. Some of these clays, such as $Mg(OH)_2$-coated bentonite and silylated palygorskite, have hydroxyl groups on their surface that can bind hydroxyl and amino groups containing reactive dyes through hydrogen bonding and Van der Waals forces. Laccase is a protein enzyme, and therefore, laccase-modified clays can electrostatically bind anionic reactive dyes.

2.1.3. Merits and demerits

The advantage of clay-type adsorbents may include their very good hydrodynamic properties and also they are cheap. However, their dye-binding capacity is not comparable to ion-exchange resins and therefore they cannot be alone effective for the complete removal of dyes from the effluent.

2.2. Ion-exchange resins

Ion-exchange resins are polymeric granules or beads with various functional groups that are capable of binding ions of opposite charge. They are either cation-exchange or anion-exchange resin but cation-exchange resins are unsuitable for the removal of reactive dyes from effluent because the dyes and resins have similar charge. Therefore, here only the anion-exchange resins have been discussed.

2.2.1. Commercial anion-exchange resins

They are the first generation adsorbents developed for the removal of dyes from textile effluent when the color of effluent became an issue around the world. A range of anion-exchange resins, such as zeolite-based Macrosorb (Crossfield), and synthetic organic polymer-based S6328 (Bayer), MP62 (Bayer), Amberlite IRC-71 (Dow), Purolite® A400 (Purolite), and Dowex (Dow), are commercially available. Of them, S6328 and MP62 [Low and Lee, 1997], and also Amberlite IRC-71 [Karcher et al., 2002], have been investigated for the removal of reactive dyes.

2.2.2. Non-commercial anion-exchange resins

A range of ion-exchange resins, such as poly(acrylic acid-N-isopropylacrylamide-trimethylolpropane triacrylate) cross-linked with sodium alginate [Dhanapal and Subramanian, 2014], partial diethylamino-ethylated cotton dust waste [Fontana et al., 2016], quaternized wood [Low et al., 2000], microcrystalline cellulose gel [El-Naggar et al., 2018], quaternized flax cellulose [Ma and Wang, 2015], cucurbit[6]uril and cucurbit[8]uril [Xie et al., 2016], porous chitosan-polyaniline/ZnO hybrid composite [Kannusamy and Sivalingam,

2013], and quaternized sugarcane bagasse [Wong et al., 2009; Aly et al., 2018], have been investigated as candidate adsorbents for the removal of reactive dyes from dyehouse effluent. Some other ion-exchange resins have been investigated that are worthy to mention may include ethylenediamine functionalised and potassium fluoride activated paper sludge [Auta and Hameed, 2014], poly(AA-NIPAAm-TMPTA) cross-linked with sodium alginate [Dhanapal and Subramanian, 2014], cellulose nanocrystal-reinforced keratin [Song et al., 2017], starch/polyaniline nanocomposite [Janaki et al., 2012], α-cellulose/polypyrrole [Ovando-Medina et al., 2015], hollow zein nanoparticles [Xu et al., 2013], lignin chemically modified with aluminum and manganese [Adebayo et al., 2014], and epichlorohydrin (ECH)-cross-linked chitosan nanoparticles [Chen et al., 2011].

2.2.3. Reactive dye removal performance of ion-exchange resins

Table 2 shows reactive dye binding capacity and the pH of maximum adsorption of reactive dyes by various ion-change resins. The commercial ion-exchange resins investigated are Bayer anion exchange resins S6328 and MP62, and also SR Amberlite IRC-718 [Karcher et al., 2002, Low and Lee, 1997]. Of them, Amberlite IRC-718 showed very poor dye binding capacity for the C.I. Reactive Blue 2 and C.I. Reactive Orange 16 [Karcher et al., 2002]. The Bayer MP62 anion-exchange resin showed excellent binding of C.I. Reactive Black 5 dye as the dye binding capacity reached 1190.14 mg g^{-1} [Low and Lee, 1997]. However, for the same dye, the Bayer S6328a ion-exchange resin showed only half of the dye binding capacity compared to the MP62 resin [Low and Lee, 1997]. Of the non-commercial resins investigated, quaternized rice husk [[Low and Lee, 1997]], and acid burnt silk cotton hull [Thangamani et al., 2007] showed quite inadequate reactive dye binding capacity. However, cellulose nanocrystal-modified keratin [Song et al., 2017] and hollow zein nanoparticles [Xu et al., 2013 showed the excellent removal of various reactive dyes from effluent and their

reactive dye binding capacity was comparable to the commercial Bayer MP62 ion-exchange resin [Low and Lee, 1997]. Thus, it will not be an exaggeration to say that some of the biomass-based ion-exchange resins developed over the years can compete with the commercial ion-exchange resins. From Table 2, it is evident that except cucurbit[6]uril, cucurbit[8]uril [Xie et al., 2016], quaternized flax cellulose [Wong et al., 2009], partial diethylamino-ethylated cotton dust waste [Fontana et al., 2016], and acid burnt silk cotton hull [Thangamani et al., 2007], all other investigated adsorbents including the high performing MP62 [Low and Lee, 1997], cellulose crystal modified with keratin [Song et al., 2017] and hollow zein nanoparticles [Xu et al., 2013] showed the maximum reactive dye binding capacity at highly acidic conditions. It is unfavorable as the pH of dyehouse reactive dyeing effluent is usually highly alkaline as the fixation of the dyestuff is carried out at pH 10.2–10.7. The pH of the effluent will need to be reduced to that level by using strong acids and after the decolorization treatment, the treated effluent will again need to be neutralized by adding alkali.

2.2.4 Reactive dye binding mechanisms

The dye binding mechanisms of chitosan and the anion-exchange resin are shown in Fig. 3. Chitosan has cationic primary amine groups, and in acidic conditions, these amine groups become positively charged due to protonation and can attract and bind anionic reactive dyes by forming ionic bonds between the sulfonate groups of dyes and amino groups of chitosan. The removal of reactive dyes by partial diethylamino-ethylated cotton dust waste, starch/polyaniline nanocomposite, and ethylenediamine-functionalized-activated paper sludge follows similar mechanism as they are also rich in amine functionalities. The ion-exchange resins have cationic quaternary ammonium or other cationic groups and can bind reactive dyes through forming ionic bonds like chitosan. On the other hand cucurbit[n]urils are

cationic exchange resins because of their esteramide groups and therefore should be unsuitable for the removal of anionic reactive dyes. However, cucurbit[8]uril showed the excellent removal of C.I. Reactive Blue 19 dye [Xie et al., 2016]. Therefore the removal could be due to hydrophobic-hydrophobic interactions and hydrogen bonding instead of ionic bonding.

2.2.4. Merits and demerits of ion-exchange resins

The ion-exchange resins are easy to handle and they can be easily recycled and reused. However, commercially available ion-exchange resins are relatively expensive and therefore a range of cheap alternatives, such as unmodified and modified cellulosic biomasses, have been extensively explored as an alternative to commercial ion-exchange resins. Ion-exchange resins are very popular, but their disposal is a problem as the synthetic ion-exchange resins are not biodegradable.

2.3. Biomass-based absorbents and their dye binding performance

Biomasses are renewable organic polymeric materials, such as plants or plant-based materials, wood, agricultural wastes, dead microbes, and material of animal origin. Biomasses can be divided mainly into three categories, namely lignocellulosic, animal, and microbial. The lignocellulosic biomasses are usually plant-based but the microbial biomasses could be dead or live microbes. Various types of biomasses have been investigated as adsorbents for the removal of reactive dyes.

2.3.1. Cellulosic biomasses and their reactive dye binding capacity

A large number of lignocellulosic biomasses, such as raw agricultural solid wastes (e.g. leaves, fibers, fruit and peel, and waste materials), have been investigated as adsorbents for binding reactive dyes [Abassi et al., 2009; Honorio et al., 2016]. The investigated solid wastes are the fruit and peel of *Trapa bispinosa*, grape fruit peel [Abassi et al., 2009], alfa fibers [Fettouche et al., 2015], Bengal gram seed husk [Reddy et al., 2017], soybean stalk, hulk and residue [Honorio et al., 2016; Gao et al., 2015; Ashori et al., 2014], eucalyptus bark [Moraisi et al., 1999], pomelo peel [Argun et al., 2014], peanut hull [Tanyildizi et al., 2011], hazelnut shell [Ferrero,2007], Brazilian pine fruit coat [Lima et al., 2008], modified wallnut shell [Cao et al., 2014], cupuassu shell [Cardoso et al., 2011a], *P. oceanica* leaf sheaths [Ncibi et al., 2007], Aqai palm (*Euterpe oleracea*) stalk [Cardoso et al., 2011b], Brazilian pine fruit shell [Cardoso et al., 2011c], pomegranate seed powder [Ghaneian et al., 2015], and waste products from forest industries including wood, bark, and sawdust [Ratnamala et al., 2016; Chakraborty et al., 2006]. These materials are abundantly available in large quantities at a very cheap price, and they could be potential dye adsorbents because of their unique physicochemical characteristics.

Table 3 shows the adsorption performance and the pH of maximum adsorption of various reactive dyes by lignocellulosic biomasses. Of the cellulosic biomasses investigated, alpha fiber powder, and soybean stalk powder, grapefruit peel, and cupuassu shell showed very poor reactive dye binding capacity [Fettouche et al., 2015; Ashori et al., 2014; Cardoso et al., 2011a]. On the other hand, modified walnut shell and soybean residue showed fairly good dye binding capacity [Gao et al., 2015; Cao et al., 2014]. The investigation of operating conditions on the dye binding capacity shows that almost all of the cellulosic biomasses show the maximum absorption at strongly acidic pH.

2.3.2. Animal-based biomasses

Chitin, a waste product of the seafood industry, could be an example of animal-based biomasses. It is a long chain polymer of *N*-acetylglucosamine, which is the primary component of cell walls of fungi, scales of fish, squid pen, and exoskeletons of crustaceans, insects, and mollusks. Chitin is inert but its deacetylated form, chitosan, is cationic and therefore has been extensively investigated as a candidate adsorbent for the removal of reactive dyes. Chitosan has been investigated as fine powder [Ignat et al., 2012; Annadurai et al., 2008], porous particles [Jiang et al., 2014; Chiou et al., 2002], flakes [Filipkowska, 2006], and films [Nga et al., 2017], for the removal of dyes. Chitin-rich squid pens have also been investigated for the removal of reactive dye [Figueiredo et al., 2000]. However, mixed results were reported for the reactive dye binding capacity of chitosan, as the dye binding capacity depends on the source and also on its molecular weight. A commercial chitosan powder showed poor dye removal but another chitosan powder made from an Indian shrimp showed the excellent removal of reactive dyes [Subramani and Thinakaran, 2000]. Various chitosan derivatives, such as ECH-cross-linked chitosan nanoparticles [Chen et al., 2011], ECH-cross-linked chitosan beads [Chiou et al., 2004], cross-linked chitosan, chitosan cross-linked with sodium edetate [Jóźwiak et al., 2015], cross-linked quaternized chitosan [Rosa et al., 2008], 3-aminopropyl-7-triethoxysilane modified chitosan beads [Vakili et al., 2015], polyethyleneimine-grafted-chitosan beads [Chatterjee et al., 2011], epichlorohydrin-cross-linked chitosan beads [Kim et al., 2012; Chiou et al., 2003], and poly(acrylamide)-grafted-chitosan [Kyzas and Lazaridis, 2009], also have been investigated as an adsorbent.

Reactive dye binding performance of chitosan derivatives

Table 4 shows the reactive dye binding capacity and the pH of maximum adsorption of reactive dyes by chitosan and its various derivatives. Of them, chitosan cross-linked with

epichlorohydrin showed an excellent removal of C.I. Reactive Black 5 and C.I. Reactive Orange 16 dyes as the dye binding capacity reached 5572.0 and 5392 mg g^{-1} respectively [Vakili et al., 2015], almost four times of the dye binding capacity shown by the high-performing commercial Bayer MP62 ion-exchange resin. The same adsorbents also showed the excellent removal of C.I. Reactive Red 189 and C.I. Reactive blue 2 dyes [Chiou et al., 2002; Chiou et al., 2004], and the maximum removal of dyes occurred at pH 2, similar to the removal of reactive dyes by the MP62 resin. Chitosan cross-linked with sodium edetate also showed reasonably high dye binding capacity and the maximum removal occurred at pH 4 [Jóźwiak et al., 2015]. It is evident that unmodified chitosan showed the maximum dye binding at near to neutral pH but the chemically modified chitosan showed the maximum binding at highly acidic conditions.

2.3.3. Color removal by microbial biomasses

Microbial biomasses, dead or living, have been extensively investigated for the removal of reactive dyes in the effluent. Microbial biomass can include bacteria, fungi, and micro-algae. They can absorb dye molecules or the enzymes secreted by them can degrade chromophores of dye molecules causing their decolorization. The investigated bacteria are *E. coli* [Kim et al., 2016], *Nostoc linckia* [Mona et al., 2011], *Lemna gibba* [Guendouz et al., 2016], *Corynebacterium glutamicum,* and *Corynebacterium glutamicum* discharged from an industrial lysine fermentation plant [Won et al., 2008; Vijayaraghavan and Yun, 2007; Won et al., 2006], a mixture of *Alcaligenes faecalis* and *Commomonas acidovorans* [Oxspring et al., 1996], *Paenibacillus azoreducens* sp. nov. [Meehan et al., 2001], *Pseudomonas luteola*, [Chang et al., 2001; Chang et al., 2000] *Lysinibacillus sp.*, and *Desulfovibrio desulfuricans* [Kim, 2007], and *Pseudomonas luteola* free cells [Hu, 1996]. Other than unmodified bacteria,

esterified bacteria and *Lysinibacillus sp.*-attached electrospun polysulfone mat [San Keskin et al., 2015], have also been investigated as an adsorbent.

A range of fungi, including dead wood-rotting fungus (*Trametes versicolor*) [Binupriya et al., 2007], *Rhizopus arrhizus* [Aksu and Cagatay, 2006; Aksu and Tezer, 2000], *Aspergillus parasiticus* [Akar et al., 2009], *Thamnidium elegans* [Akar et al., 2017], fungal strain VITAF-1 [Sinha and Osborne, 2016], *Rhizopus nigricans* [Kumari and Abraham, 2007], *Penicillium ochrochloron* [Aytar et al., 2016], *Rhizopus nigricans* and *Penicillium restrictum* [Iscen et al., 2007], *Termitomyces clypeatus* [Bagchi and Ray, 2015], *Aspergillus versicolor* [Kara et al., 2012], *Aspergillus niger* [Bagchi and Ray, 2015] and *Symphoricarpus albus* [Kara et al., 2012], mixed *Aspergillus versicolor* and *Rhizopus arrhizus* with dodecyl trimethylammonium bromide,[Gül and Dönmez, 2013] *Phanerochaete chrysosporium*,[Dharajiya et al., 2016] *Aspergillus fumigatus*,[Dharajiya et al., 2016] mixed cultures isolated from textile effluent,[Çetin and Dönmez, 2006] and *Aspergillus fumigatus* isolated from textile effluent,[Karim et al., 2017] have been investigated as a candidate adsorbent for the removal of reactive dyes. Also, several algae, including *Spirulina platensis* [Cardoso et al., 2012], *Enteromorpha prolifera* [Sun et al., 2013], and *Chlorella vulgaris* [Aksu and Tezer, 2005], have been investigated for the removal of reactive dyes.

Dye binding capacities of microbial biomasses

Table S2 (Supplementary Content) shows the list of bacteria investigated for the removal of color and their dye absorption performance. Mona et al. investigated *Nostoc linckia* bacterium for the removal of C.I. Reactive Red 120 and found that absorption carried out at 35 °C showed higher dye absorption (422.5 mg g^{-1}) compared to the absorption carried out at 25 °C [Mona et al., 2011]. Some of the bacteria investigated for the decolorization of reactive

dyes, such as *Lemna gibba* [Guendouz et al., 2016], and *Escherichia coli* [Kim et al., 2016], showed quite poor dye removal at as low as 6.13 mg g^{-1} [Guendouz et al., 2016]. On the other hand, raw and esterified *E. coli* [Guendouz et al., 2016], and *Corynebacterium glutamicum* [Kim et al., 2016], showed excellent reactive dye binding capacity. Most of the bacteria investigated showed the highest dye binding capacity at pH 1-3 [Akar et al., 2017; Sinha and Osborne, 2016], except *Pseudomonas luteola* free cells and *Desulfovibrio desulfuricans*. They showed the maximum removal at neutral to alkaline pH.

Of the fungi investigated, *Aspergillus versicolor*, *Termitomyces clypeatus*, *Aspergillus niger*, and *Symphoricarpus albus* showed relatively poor reactive dye binding capacity. However, VITAF-1 and *Rhizopus nigricans* showed quite good dye binding capacity. Unlike bacteria, fungi show their dye binding capacity at a broad pH (1-8) [Aytar et al., 2016; Gül and Dönmez, 2013; Dharajiya et al., 2016]. All of the fungi showed quite a poor removal of the dye except *Rhizopus arrhizus* and VITAF-1. Of the fungal biomasses, *Rhizopus* (*Rhizopus arrhizus*) showed the highest reactive dye binding capacity for both C.I. Reactive Black 5 and C.I. Reactive Blue 21 dyes (501 and 773 mg g^{-1} respectively) when the treatment was carried out at 35 and 45 °C respectively at pH 2. Won et al. investigated *Rhizopus oryzae* in combination with *Aspergillus versicolor* with or without cetyltrimethylammonium bromide (CTAB) for the removal of C.I. Reactive Blue 19, but found that 100% decolorization took 6 days when the decolorization treatment was carried out in the presence of CTAB [Won et al., 2006]. Without CTAB, the color removal efficiency dropped to 86% for the same time period. Other than bacteria and fungi, microalgae also have been investigated as adsorbents. Of them, *Spirulina platensis* [Cardoso et al., 2012], and *Enteromorpha prolifera* [Sun et al., 2013], showed some levels of reactive dye binding capability. Although *Chlorella vulgaris* showed quite a good removal of C.I. Reactive Black 5, for the C.I. Reactive Orange 107 the binding capacity was very poor [Aksu and Tezer, 2005].

2.3.4 Reactive dye binding mechanisms

Lignocellulosic biomasses have many hydroxyl groups. The reactive dyes are removed by forming hydrogen bonds with hydroxyl groups of these constituents and also through Van der Waals forces. The removal of reactive dyes by animal-based biomasses occurs mainly due to the forming of ionic bonds between the sulfonate groups of dyes and the amino groups of the adsorbents. However, the removal of color by bacterial cells mainly occurs by the physical adsorption of dye molecules into bacterial cells [Bras et al., 2001]. The color removal efficiency is diffusion dependent, and when the surface of a cell is saturated with dye molecules, the adsorption of dye molecules stops. The disadvantages of bacterial biomass adsorption based treatments include the difficulty of removing the adsorbents from the treated water, and also recovered biomass will need to be disposed of. Therefore, degradation of the dyestuffs could be favorable as they permanently remove the color. Reactive dyes are quite large molecules and also have substituent sulfonate groups. Therefore, reactive dye molecules will be unlikely absorbed into the cells by passing through the cell membrane and therefore the dye removal is not dependent on the intracellular uptake of the dye [Robinson et al., 2001]. The adsorbed dye could be reduced by enzymes (such as cytoplasmic flavin-dependent azoreductases) produced by bacterial cells [Robinson et al., 2001]. Pearce et al. opine that electron transport-linked reduction could be responsible for the reduction of dyes in the extracellular environment [Pearce et al., 2003]. During the metabolism of the certain substrate, bacteria form low molecular weight redox mediator compounds that can act as electron shuttles between the azo dye and a nicotinamide adenine dinucleotide (NADH)-dependent azoreductase that is available in the outer membrane [Gingell and Walker, 1971]. In an anaerobic condition, the addition of anthraquinone sulphonate can facilitate the non-enzymatic reduction of azo chromophores [Plumb et al., 2001]. Therefore, the removal of

dyes by bacteria could be a combination of adsorption and reduction process. The removal of color by microbial biomasses is advantageous as the absorbed dyes are degraded unlike any other type of adsorbent.

2.3.5. Merits and demerits of biomass adsorbents

The main advantages of biomass-based adsorbents may include their easy disposal because of their high biodegradability and low cost. However, the poor dye binding capacities shown by various cellulosic biomasses indicates that they cannot compete with the commercial ion-exchange resins. The main constituents of cellulosic biomass are cellulose, hemicellulose, lignin, and polyphenols and all of them are weakly anionic. Because of their weakly anionic nature, cellulosic adsorbents are not a good adsorbent for the removal of anionic reactive dyes. On the other hand, chitosan is cationic and therefore it can bind reactive dyes by forming ionic bonding. It can be concluded that cross-linked and quaternized chitosan derivatives are promising adsorbents that can replace commercial ion-exchange resins for the removal of reactive dyes from the effluent. However, the use of chitosan as a dietary supplement has increased its price. The key challenges of removal of dyes by biosorption are the difficulties in procurement and transportation of high volume of biomasses, poor hydrodynamic properties, poor recyclability and their removal from the treated effluent.

2.4. Magnetic ion-exchange adsorbents and their reactive dye binding performance

2.4.1. Magnetic ion-exchange adsorbents

The high removal of color by an adsorbent is not enough, as the separation of biosorbent from the treated water is cumbersome. Therefore, recent research has emphasized the ease of separation of adsorbent from the treated effluent, resulting in the development of magnetic nanoparticles. By using a strong magnet, the used adsorbent can be easily separated. The investigated magnetic nanoparticles may include laccase immobilized epoxy-functionalized magnetic chitosan beads [Bayramoglu et al., 2010], magnetic chitosan microparticles functionalised with polyamidoamine dendrimers [Wang et al., 2015], magnetic N-lauryl chitosan particles [Debrassi et al., 2012], glutaraldehyde (GLA) cross-linked magnetic chitosan nanoparticles [Elwakeel et al., 2009], chitosan-based magnetic microspheres [Xu et al., 2018], glutaraldehyde cross-linked magnetic chitosan nanocomposites [Kadam and Lee, 2015], modified magnetic chitosan microspheres [Jafari et al., 2016], quaternized magnetic resin microspheres [Li et al., 2014], magnetic carbon nanotube-κ-carrageenan-Fe_3O_4 nanocomposite [Duman et al., 2016], quaternized magnetic microspheres [Shuang et al., 2012], O-carboxymethyl chitosan-N-lauryl/γ-Fe_2O_3 magnetic nanoparticles [Demarchi et al., 2015], L-arginine-functionalized Fe_3O_4 nanoparticles [Dalvand et al., 2016], and magnetic Fe_3O_4/chitosan nanoparticles [Cao et al., 2015]. The nanoparticles are mostly made magnetic by forming either Fe_2O_3 or Fe_3O_4 nanoparticles in-situ within the organic or inorganic nanoparticles.

2.4.2. Reactive dye binding capacity and dye binding mechanisms

Table 5 shows the reactive dye binding capacity of various organic magnetic nanoparticles investigated as a candidate adsorbent for the removal of reactive dyes from the effluent. Of the magnetic nanoparticles investigated, only a few of them show some levels of potential as adsorbents. Of them, laccase immobilized magnetic chitosan beads showed very poor dye-binding capacity as the adsorbent showed only 2.05 and 1.42 mg g^{-1} dye adsorption in the

case of C.I. Reactive Yellow 2 and C.I. Reactive Blue 4 respectively [Bayramoglu et al., 2010]. Magnetic carbon nanotube-κ-carrageenan-Fe_3O_4 nanocomposite also showed relatively low dye binding capacity but considerably higher than the dye binding capacity shown by laccase immobilized magnetic chitosan beads [Duman et al., 2016]. Of the magnetic nanoparticles investigated, quaternized magnetic resin microspheres and quaternized GLA-cross-linked magnetic chitosan particles showed some reasonable levels of dye binding capacity, 773.6 and 936.6 mg g^{-1} for the C.I. Reactive Black 5 and C.I. Reactive Red 120 dyes, respectively at highly acidic conditions (pH 2) [Elwakeel et al., 2009; Shuang et al., 2012]. It is evident that the formation of magnetic nanoparticles within the pores of organic micro/nanoparticles substantially reduces their porosity and pore volume, which affects their dye binding performance, as the magnetic particles of chitosan showed much lower dye binding capacity compared to the ECH-cross-linked chitosan. They are not practical for the removal of dyes as the cost of production of these adsorbents will be relatively high and the levels of removal achieved are only one-third of the dye binding capacity shown by activated carbon. The challenges of magnetic nanoparticles are the non-availability of these adsorbents at an economical price, low reactive dye binding capacity, poor decolorization efficiency and the economic regeneration of the adsorbents.

The magnetic ion-exchange adsorbents bind dye molecules having opposite charge and also can bind dye molecules having hydroxyl and amino groups through hydrogen and Van der Waal's bondings.

2.4.4. Merits and demerits of magnetic ion-exchange adsorbents

The key advantage of magnetic ion-exchange adsorbents is their easy removal from the treated effluent. However, they show relatively poor dye binding capacity compared to the other adsorbents investigated.

3. Effect of functional and substituent groups on dye adsorption capacity

The reactive dyes have one or more than one anionic groups (usually sulfonic acid groups) and also some dyes have substituent groups, such as alkyl, amino, and acetamide groups. They may have an effect on their adsorption by ion-exchange type adsorbents. Auta and Hameed investigated the removal of two reactive dyes, C.I. Reactive Orange 16 and also C.I. Reactive Blue 19 by the functionalized paper sludge [Auta and Hameed, 2014]. Both of the dyes have two sulfonic acid groups in their structure but the removal of C.I. Reactive Orange 16 dye was better than the other dye, which has a cationic amino functional group. The cationic substituent group affected its absorption by the activated paper sludge. Starch aniline composites have been investigated for the removal of C.I. Reactive Black 5 and C.I. Reactive Violet 4 [Janaki et al., 2012]. The removal of four sulfonate groups-containing C.I. Reactive Black 5 was considerably better than the other dye, which has three sulfonate groups and a hydrophobic acetamide group that affected its adsorption into the cationic starch adsorbent. Similarly, in the case of sodium edetate cross-linked chitosan, the adsorption of six sulfonate groups-containing C.I. Reactive yellow 84 was 50% higher than the four sulfonate groups containing C.I. Reactive Black 5 [Jóźwiak et al., 2015]. In the case of ECH-cross-linked chitosan, four sulfonate groups-containing C.I. reactive Black 5 showed better adsorption than the two sulfonate groups-containing C.I. Reactive Orange 16. However, in the case of nanoporous (pore size = 2.9 nm) quaternized magnetic resin microparticles, six sulfonate groups-containing C.I. Reactive Red 120 absorbed less than two-sulfonate groups containing C.I. Reactive orange 16 [Shuang et al., 2012]. The molecular weight of C.I. Reactive Orange 16 is 617.526 but the molecular weight of C.I. Reactive Red 120 is 1469.98, more than double of the molecular weight of the other dye. The high molecular weight of C.I. Reactive

Red 120 affected its adsorption into the nanoporous magnetic resin particles. Therefore, it is evident that the reactive dye adsorption by various ion-exchange type adsorbents is affected not only by the number of anionic groups in the dye but also by their molecular weight and the substituent groups present in the dye molecules.

As mentioned before that the dye adsorption between the ion-exchange resin and reactive dyes depends on the ionic attractions between the cationic resins and anionic reactive dyes. The increase in anionic groups in reactive dyes increases the attraction between the dye and the anion-exchange resin. On the other hand, when dyes have cationic substituent groups (amine or amide), they affect this ionic attraction as the dyes and the resin both become cationic resulting in affecting the adsorption of the dye molecules.

4. Synthesis of anion-exchange resins

Ion-exchange resins are mainly synthesized by addition and condensation polymerizations. Condensation polymerization method is rarely used for the synthesis of anion-exchange resin but it is used for the synthesis of cation-exchange resin. A terpolymer of p-hydroxybenzaldehyde, biuret and formaldehyde could be an example of the formation of the ion-exchange resin prepared by condensation polymerization as shown in Fig. S2 (Supplementary content) [Patle and Gurnule, 2016]. The synthesis of anion-exchange resin from 2-methyl-5-vinylpyridine and divinylbenzene could be an example of addition polymerization. Cross-linked polyvinyl methyl pyridine is prepared by the addition polymerization of 2-methyl-5-vinylpyridine in the presence of divinylbenzene, which is used as a crosslinking agent [Vorotyntsov et al., 2018]. The polystyrene beads are then chloromethylated followed by amination, which introduces cationic groups in the resin making them anion-exchange resin. Addition polymerization is popular as the

polymerization reaction progress rapidly and at a lower temperature compared to the compared to the condensation polymerization method. The addition polymerization proceeds in chain growth pattern but the condensation polymerization proceeds with the step-growth pattern. In addition polymerization, only one monomer is needed to form a polymer but for the condensation polymerization, at least two monomers are needed. Ion-exchange resins formed by condensation polymerization are not stable at alkaline pH as C-O and C-N links are susceptible to hydrolytic cleavages [Craig, 1953]. On the other hand, ion-exchange resins prepared by addition polymerization is quite stable over wide range of pHs and temperatures used in ion-exchange adsorptions as they mainly have C-C bonds in the macromolecular chains [Craig, 1953]. As the produced adsorbent is water-insoluble and therefore it is easy to separate them from the effluent.

Anion-exchange resins can be produced by various methods including chemical modifications, polymeric grafting and also by crosslinking as mentioned below:

41. Copolymerization and crosslinking

This is the most common method used for the synthesis of ion-exchange resins and mostly polymerization and crosslinking are carried out in a single step. In this case, cationic monomers are polymerized and cross-linked to form water-insoluble anion-exchange resins. Quaternary ammonium, polyamine, etc., are popular polymers for making this kind of anion-exchange resins. On the other hand, an anion-exchange resin usually contains amine or quaternary ammonium groups, such as poly(vinyl benzyl trimethyl-ammonium chloride-co-vinyl benzene) anion-exchange resin, which is produced by the free-radical copolymerization of (vinyl benzyl)trimethylammonium chloride with divinylbenzene (Fig. 4). The merits may

include that the synthesized adsorbents become water-insoluble and also it is easy to control the porosity of the adsorbents by controlling the crosslinking density. Another example could be XUS 43600.00 commercialized by Dow Chemicals which made from divinylbenzene cross-linked chloromethylated styrene and functionalization with bis-picolylamine functional groups. Most of these adsorbents are not eco-friendly as they are not biodegradable.

4.2. Crosslinking of a single polymer

In this method, a single cationic polymer is cross-linked by covalent bond forming or ionic bond forming crosslinking agents. For example, chitosan beads are prepared by using various crosslinking agents including covalent bond forming glutaraldehyde and epichlorohydrin and ionic bond, forming tripolyphosphate and sodium edetate. Fig. 5 shows the crosslinking of chitosan by using covalent bond forming epichlorohydrin and glutaraldehyde crosslinking agents as well as the ionic crosslinking with sodium edetate and trisodium citrate. This is a cheaper technique to make ion-exchange resin than other methods as only needs to carry out the crosslinking reactions, which converts the water-soluble polymer into the water-insoluble ion-exchange resin. This method is mainly used for the production of anion-exchange resins from bio-based and biodegradable polymers.

4.3. Chemical modification of polymers

The polymers having hydroxyl, carboxyl, thiol or amino groups can be easily converted into an anion-exchange resin by chemical modifications. For example, sugarcane bagasse is a

cellulosic material, which can be converted quaternary cellulose by reacting with a quaternary ammonium compound, such as 2,3-epoxypropyltrimethylammonium chloride [Hassan, 2014]. Fig. 6 (top) shows the mechanism of formation of quaternary ammonium chitosan and cellulose by reacting with an epoxy group-containing quaternary ammonium compound. The quaternary ammonium groups are strongly cationic and therefore they can act as an anion-exchange resin. It is also one of the cheap methods for the synthesis of anion-exchange resin and it is easy to separate the resins after the adsorption treatment.

4.4. Polymeric grafting

Graft-copolymerization is an important tool to modify the surface functionalities to make them either cationic or anionic, which is used to modify various lignocellulosic and carbonaceous adsorbents. Cationic polymers (e.g. polymers containing amine or quaternary ammonium groups, polyaniline, polypyrrole) are grafted onto cellulose macromolecular chain to introduce cationic functionalities to make them anionic-exchange resin. Cellulosic materials contain a large number of hydroxyl groups (they are weakly anionic) and therefore it is advantageous to make them anionic exchange resin as the unsubstituted hydroxyl groups also will take part in the anion exchange. On the other hand, if a cellulosic material is converted into the anion-exchange resin, these unsubstituted hydroxyl groups will have a negative impact on their cationic exchange. For example, Fig. 6 (bottom) shows the formation of quaternized chitosan and cellulose by grafting a quaternary ammonium polymer onto their macromolecular chains [Hassan, 2015]. The synthesis of the adsorbent by this method is more expensive compared to the second and the third method, and the produced resins could be water soluble making their removal from the effluent cumbersome.

5. Modeling of adsorption process

5.1. Modeling of adsorption isotherm

Adsorption of reactive dyes by various adsorbents can be expressed by various isotherm models. Adsorption isotherms are used to describe the interaction between the dye molecules, dye adsorption equilibrium, and the dye binding active sites of the adsorbents [Cao et al., 2015]. Adsorption isotherm expresses the amount of adsorbate on the absorbent surface as a function of its concentration at a constant temperature. Adsorption process of dyes can be described by various empirical adsorption isotherm models including Langmuir, Freundlich, Temkin, Dubinin–Radushkevich, Redlich-Peterson, and Sips. They are used to predict the adsorption capacities of reactive dyes by activated carbon and to fit the experimental equilibrium data. According to Freundlich model, adsorption takes place at specific heterogeneous surfaces and the linear form of this model is represented as [Freundlich, 1906, Vijayaraghavan et al., 2006]:

$$\ln q_e = \ln K_F + \frac{1}{n} \ln C_e \qquad [1]$$

where K_F (l g^{-1}) and n (dimensionless) are Freundlich isotherm constants which represent the adsorption and the degree of nonlinearity between solution concentration and adsorption, respectively. A plot of ln q_e vs ln C_e would result in a straight line with a slope of 1/n and intercept of ln K_F. For example, the adsorption of reactive dyes by ion-exchange type adsorbents is mainly represented by the Langmuir isotherm model and the kinetic data usually follow the pseudo-second-order model. For example, Fig. 7 shows Langmuir and Freundlich isotherm models for the adsorption of C.I. Reactive Blue 19 onto hollow zein

nanoparticles and C.I. Reactive Red 45 onto S. albus bacteria [Xu et al., 2013, Kara et al., 2012]

The Temkin isotherm model, like Freundlich model, is one of the earliest isotherm models, which was developed to describe the adsorption of hydrogen atom onto platinum electrodes in an acidic aqueous solution. In the Temkin adsorption isotherm equation, the energy of adsorption is a linear function of surface coverage. This adsorption model is only valid for medium ion concentrations. The linear form of the model is as follows [[Samarghandi et al., 2009]]:

$$q_e = \frac{Rt}{b} \ln K_T + \frac{RT}{b} \ln C_e \qquad [2]$$

where b is a Temkin constant which is related to the heat of sorption (J mol^{-1}) and K_T is a Temkin isotherm constant (l mg^{-1}) [Langmuir, 1916]. Fig S3 (Supplementary Content) shows that the removal C.I. Reactive Red 120 by industrial lignin can be described by Temkin isotherm model [Suteu et al., 2010]. On the other hand, Langmuir model is based on four assumptions: all of the adsorption sites are equivalent and each site can only accommodate one molecule, the surface is energetically homogeneous and adsorbed molecules do not interact, there are no phase transitions, and at the maximum adsorption, only a monolayer is formed [Dubinin and Radushkevich, 1947]. Adsorption only occurs on localized sites on the surface, not with other adsorbates. The linear form of the Langmuir model can be represented as:

$$\frac{C_e}{q_e} = \frac{1}{q_{max}} + \left(\frac{1}{q_{max} \times K_L}\right) \times \frac{1}{C_e} \qquad [3]$$

The Dubinin–Radushkevich model has been widely used to correlate adsorption isotherms following a pore filling mechanism on activated carbons and other microporous adsorbents [Redlich and Peterson, 1959]. Other previous models could not accurately describe the

adsorption of adsorbate into microporous adsorbents. The linear form of the model can be represented as:

$$\ln q_e = \ln q_s - K_D \varepsilon^2 \quad [4]$$

$$\varepsilon^2 = RT \ln\left(1 + \frac{1}{C_e}\right) \quad [5]$$

where q_s (mg P g^{-1}) is constant in the Dubinin–Radushkevich model, which is related to the absorption capacity. K_D ($mol^2\ kJ^{-2}$) is a constant related to the mean free energy of the absorption. For example, Fig. S4 shows that the adsorption of C.I. Reactive Orange 16 by waste sunflower seed shells follows the Dubinin–Radushkevich model [Suteu et al., 2011].

The Redlich-Peterson (R-P) isotherm is a three-parameter empirical adsorption model that incorporates elements from both the Langmuir and Freundlich isotherms and improves the inaccuracies [Sips, 1948]. The adsorption mechanism is unique, which does not follow ideal monolayer adsorption characteristics. The linear form of the isotherm model can be expressed as:

$$\ln\left(K_R \frac{C_e}{q_e} - 1\right) = g \ln C_e + \ln a_R \quad [6]$$

Sips model is a three-parameter isotherm model, which is combined a form of Freundlich and Langmuir expressions deduced for predicting the heterogeneous adsorption [Gunay et al., 2007]. The linear form of the model can be expressed as [Toth, 1971]:

$$\beta_S \ln C_e = -\ln\left(\frac{K_S}{q_e}\right) + \ln a_S \quad [7]$$

It was reported that the removal of the C.I. Reactive Black 5 by Brazilian pine fruit shell followed Sips adsorption isotherm model but the activated carbon made from it followed the Redlich-Peterson model as shown in Fig. S5 (Supplementary Content) [Cardoso et al., 2010c].

5.2. Kinetic models

Kinetic models are utilized to determine the mechanism of sorption process including the rate of adsorption, diffusion control, and mass transfer. Depending on the rate of adsorption, reaction kinetics could be first order and second order. Legergen proposed a first-order rate of reaction to describe the kinetic process of liquid-solid phase adsorption of oxalic acid and malonic acid onto charcoal [Ho, 2004], which is probably the first model to describe the rate of adsorption. The equation as:

$$\frac{d(q_t)}{dt} = k_1(q_e - q_t) \qquad [9]$$

Where q_e and q_t are the amounts of dye adsorbed (mg g^{-1}) at the equilibrium and at the time t (min), respectively, and k_1 is the pseudo-first order rate constant (min^{-1}). If the eq. 1 is integrated with the boundary conditions of $q_t = 0$ at t=0 and $q_t=q_t$ at t=t, then the equation can be written as [Ho, 1996]:

$$\ln\left(\frac{q_e}{q_e - q_t}\right) = k_1 t \qquad [10]$$

By rearranging equations 1 and 2, the pseudo-first-order equation can be expressed as

$$\log(q_e - q_t) = \log\ q_e - \frac{k_1}{2.303} t \qquad [11]$$

In 1995, a new kinetic model was proposed to describe the kinetics of divalent metal ion uptake onto peat as the uptake followed the second order of reaction [Ho, 1996]. The equation can be written as:

$$\frac{dq_t}{dt} = k_2(q_e - q_t)^2 \qquad [12]$$

where q_e and q_t are the numbers of active sites occupied at the equilibrium and at the time t (min), respectively, and k_2 is the pseudo-second-order rate constant (g mg^{-1} min^{-1}). If the eq. 11 is integrated with the boundary conditions of $q_t = 0$ at t=0 and $q_t=q_t$ at t=t and rearranging, the pseudo-second-order sorption rate can be written as:

$$\frac{t}{q_t} = \frac{1}{k_t q_e^2} + \frac{1}{q_e} \qquad [13]$$

where k_2 is the pseudo-second-order rate constant (g mol^{-1} min^{-1}), and initial sorption rate (h) is equal to $k_t q_e^2$ ((g mol^{-1} min^{-1}). These two equations are mostly used to describe the adsorption of reactive dyes by various adsorbents. For example, it was reported that the adsorption of C.I. Reactive Blue 19 onto L-arginine-functionalized Fe_3O_4 nanoparticles followed pseudo-first-order and pseudo-second-order reaction rates as shown in Fig. S6 (Supplementary Content) [Dalvand et al., 2016].

6. Conclusions and future directions

In this review, the research carried out using various ion-exchange resin-like adsorbents including modified clays, lignocellulosic biomasses, chitosan and its derivatives, microbial biomasses and magnetic particles investigated over the years for the treatment of dyehouse effluent containing reactive dyes have been critically discussed. The dye binding capacities of

various types of adsorbents under different operating conditions are compared. The last decade has seen interest in developing biobased adsorbents as alternatives to activated carbon, especially lignocellulosic biomasses for the treatment of dyehouse effluent. However, the success achieved for the removal of reactive dyes is very limited because of their poor hydrodynamic properties, limited recycling and reusability, unpredictable adsorption behavior, and difficulty in regeneration compared to the activated carbon adsorbents. Some of the adsorbents, such as lignocellulosic adsorbents, investigated for the removal of reactive dyes showed poor dye binding capacity as the adsorbents and reactive dyes both are anionic. On the other hand, cationic chitosan showed excellent reactive dye-binding capacity. The literature survey shows that various cross-linked (such as epichlorohydrin and edetate) and quaternized chitosan provide the highest removal of reactive dyes. The synthesis methods of various ion-exchange adsorbents and chitosan derivatives are described. The dye binding capacity is affected by the molecular weight of the dyes and also by the functional groups of dyes. The adsorption of dyes into the adsorbents is affected by the adsorption time, pH, temperature, adsorbent dosage, the initial concentration of the dye in the effluent, and the type of adsorbent.

Almost all of these adsorbents have been investigated for the batch study using simulated reactive dye effluents but in industry, effluent treatment needs to be carried out in continuous mode. Therefore, further research will need to be carried out to determine their suitability for the continuous treatment of effluent. The adsorption treatments produce sludge, which needs to be treated before their disposal. Therefore, appropriate treatment for the disposal of sludge also will need to be developed.

Acknowledgment

The authors acknowledge the financial support received from the Ministry of Business, Innovation, and Employment of New Zealand through Grant No. C10X0824.

References

Abassi, M., Asl, N.R., 2009. Removal of hazardous reactive blue 19 dye from aqueous solution by agricultural waste. J. Iran. Chem. Res. 2, 221–230.

Adebayo, M.A., Prola, L.D.T., Lima, E.C., Puchana-Rosero, M.J., Cataluña, R., Saucier, C., Umpierres, C.S., Vaghetti, J.C.P., da Silva, L.G., Ruggiero, R., 2014. Adsorption of Procion Blue MX-R dye from aqueous solutions by lignin chemically modified with aluminium and manganese. J. Hazard. Mater. 268, 43–50.

Adsorptive removal of anionic dyes by chitosan-based magnetic microspheres with pH-responsive properties. J. Mol. Liquid. 256, 424–432.

Aguiar, J.E., Bezerra, B.T.C., Braga, B.M., Lima, P.D.S., Nogueira, R.E.F.Q., de Lucena, S.M.P., José da Silva Jr., I., 2013. Adsorption of anionic and cationic dyes from aqueous solution on non-calcined mg-al layered double hydroxide: experimental and theoretical study. Separat. Sci.Technol. (Philadelphia) 48, 2307–2316.

Akar, T., Sayin, F., Turkyilmaz, S., Tunali Akar, S., 2017. The feasibility of *Thamnidium elegans* cells for color removal from real wastewater. Process Safety Environ. Protect. 105, 316–325.

Akar, S. T., Akar, T., Çabuk, A., 2009. Decolorization of a textile dye, Reactive Red 198 (RR198), by *Aspergillus parasiticus* fungal biosorbent. Brazilian J. Chem. Eng. 26, 399–405.

Aksu, Z., Cagatay, S.S., 2006. Investigation of biosorption of Gemazol Turquoise Blue-G Reactive dye by dried Rhizopus arrhizus in batch and continuous systems. Sep. Purif. Technol. 48, 24–35.

Aksu, Z., Tezer, S., 2000. Equilibrium and kinetic modeling of biosorption of Remazol Black B by Rhizopus arrhizus in a batch system: effect of temperature. Process Biochem. 36, 431–9.

Aksu, Z., Tezer, S., 2005. Biosorption of reactive dyes on the green alga Chlorella vulgaris. J. Process Biochem. 40, 1347–1361.

Aly, A.A., Mahmoud, S.A., El-Apasery, M.A., 2018. Decolorization of reactive dyes. Part I. Eco-friendly approach of reactive dye effluents decolorization using cationized sugarcane bagasse. Pigment Resin Technol. 47, 108–115.

Amin, M.T., Alazba, A.A., Shafiq, M., 2015. Adsorptive removal of reactive black 5 from wastewater using bentonite clay: isotherms, kinetics and thermodynamics. Sustainability 7, 15302–15318.

Annadurai, G., Ling, L.Y., Lee, J.-F., 2008. Adsorption of reactive dye from an aqueous solution by chitosan: Isotherm, kinetic and thermodynamic analysis. J. Hazard. Mater. 152, 337–346.

Annual Report 2016-17, 2017. Department of Chemical and Petrochemicals, Ministry of Chemicals & Fertilizers, Government of India.

Argun, M.E., Guclu, D., Karatas, M., 2014. Adsorption of Reactive Blue 114 dye by using a new adsorbent: Pomelo peel. J. Ind. Eng. Chem. 20, 1079–1084.

Ashori, A., Hamzeh, Y., Ziapour, A., 2014. Application of soybean stalk for the removal of hazardous dyes from aqueous solutions. Polym. Eng. Sci. 54, 239–245.

Asouhidou, D.D., Triantafyllidis, K.S., Lazaridis, N.K., Matis, K.A., 2012. Adsorption of reactive dyes from aqueous solutions by layered double hydroxides. J. Chem. Technol. Biotechnol. 87, 575–582.

Auta, M., Hameed, B.H., 2014, Optimized and functionalized paper sludge activated with potassium fluoride for single and binary adsorption of reactive dyes. J. Ind. Eng. Chem. 20, 830–840.

Aytar, P., Bozkurt, D., Erol, S., Özdemir, M., Çabuk, A., 2016. Increased removal of Reactive Blue 72 and 13 acidic textile dyes by Penicillium ochrochloron fungus isolated from acidic mine drainage. Desalin. Water Treat. 57, 19333–19343.

Bagchi, M., Ray, L., 2015. Adsorption behavior of Reactive Blue 4, a triazine dye on dry cells of Rhizopus oryzae in a batch system. Chem. Speciat. Bioavail. 27, 112–120.

Bayramoglu, G., Yilmaz, M., Arica, M.Y., 2010. Preparation and characterization of epoxy-functionalized magnetic chitosan beads: Laccase immobilized for degradation of reactive dyes. Bioprocess Biosys. Eng. 33, 439–448.

between the effects of nitrate, phosphate, boron and heavy metals on charophytes. New Phytol. 189, 1051–1059.

Bharathi, K.S., Ramesh, S.T., 2013. Removal of dyes using agricultural waste as low-cost adsorbents: a review. Appl. Water Sci. 3, 773–790.

Binupriya, A.R., Sathishkumar, M., Dhamodaran, K., Jayabalan, R., Swaminathan, K., Yun, S.E., 2007. Liquid-phase separation of reactive dye by wood-rotting fungus: A biotechnological approach. Biotechnol. J. 2, 1014–1025.

Bras, R., Ferra, I.A., Pinheiro, H.M., Goncalves, I.C. Batch tests for assessing decolorization of azo dyes by methanogenic and mixed cultures. J. Biotechnol. 2001, 89, 155–162.

Cao, C., Xiao, L., Chen, C., Shi, X., Cao, Q., Gao, L., 2014. In situ preparation of magnetic Fe_3O_4/chitosan nanoparticles via a novel reduction–precipitation method and their application in adsorption of reactive azo dye. Powder Technol. 260, 90–97.

Cao, J.S., Lin, J.X., Fang, F., Zhang, M.T., Hu, Z.R., 2014. A new absorbent by modifying walnut shell for the removal of anionic dye: kinetic and thermodynamic studies. Bioresour. Technol. 163, 199–205.

Cardoso, N. F., Lima, E. C., Calvete, T., Pinto, I. S., Amavisca, C. V., Fernandes, T. H. M., Pinto, R.B., Alencar, W.S., 2011b. Application of aqai stalks as biosorbents for the removal of the dyes Reactive Black 5 and Reactive Orange 16 from aqueous solution. J. Chem. Eng. Data 56, 1857–1868.

Cardoso, N. F., Pinto, R., Lima, E. C., Pinto, I. S., 2011c. Removal of Remazol Black B textile dye from aqueous solution by adsorption. Desalin. 269, 92–103.

Cardoso, N.F., Lima, E.C., Pinto, I.S., Amavisca, C.V., Royer, B., Pinto, R.B., Alencar, W. S., Pereira, S.F.P., 2011a. Application of cupuassu shell as biosorbent for the removal of textile dyes from aqueous solution. J. Environ. Manage. 92, 1237–1247.

Cardoso, N.F., Lima, E.C., Royer, B., Bach, M. V., Dotto, G.L., Pinto, L.A.A., Calvete, T., 2012. Comparison of Spirulina platensis microalgae and commercial activated carbon as adsorbents for the removal of Reactive Red 120 dye from aqueous effluents. J. Hazard. Mater. 241–242, 146–153.

Çetin, D., Dönmez, G., 2006. Decolorization of reactive dyes by mixed cultures isolated from textile effluent under anaerobic conditions. Enzyme Microb. Technol. 38, 926–930.

Chakraborty, S., Basu, J.K., De, S., Dasgupta, S., 2006. Adsorption of reactive dyes from a textile effluent using sawdust as the adsorbent. Ind. Eng. Chem. Res. 45, 4732–4741.

Chang, J.-S., Chou, C., Chen, S.-Y., 2001. Decolorization of azo dyes with immobilized Pseudomonas luteola. Process Biochem. 36, 757–763.

Chang, J.-S., Lin, Y.-C., 2000. Fed-batch bioreactor strategies for microbial decolorization of azo dye using a Pseudomonas luteola strain. Biotechnol. Prog. 16, 979–985.

Chatterjee, S., Chatterjee, T., Woo, S.H., 2011. Influence of the polyethyleneimine grafting on the adsorption capacity of chitosan beads for Reactive Black 5 from aqueous solutions. Chem. Eng. J. 166, 168–175.

Chen, C.-Y., Chang, J.-C., Chen, A.-H., 2011. Competitive biosorption of azo dyes from aqueous solution on the templated cross-linked-chitosan nanoparticles. J. Hazard. Mater. 185, 430-441.

Chinoune, K., Bentaleb, K., Bouberka, Z., Nadim, A., Maschke, U. Adsorption of reactive dyes from aqueous solution by dirty bentonite. Appl. Clay Sci. 2016, 123, 64–75.

Chiou, M.-S., Ho, P.-Y., Li, H.-Y., 2004. Adsorption of anionic dyes in acid solutions using chemically cross-linked chitosan beads. Dyes Pigm. 60, 69-84.

Chiou, M.-S., Kuo, W.-S., Li, H.-Y., 2003. Removal of reactive dye from wastewater by adsorption using ECH cross-linked chitosan beads as medium. J. Environ. Sci. Health A, 38, 2621–2631.

Chiou, M.-S., Li, H.-Y., 2002. Equilibrium and kinetic modeling of adsorption of reactive dye on cross-linked chitosan beads. J. Hazard. Mater. 93, 233–248.

Craig, P.N., 1953. Synthesis of ion-exchange resins. Ann. N. Y. Acad. Sci. 11, 57, 67–78.

Dalvand, A., Nabizadeh, R., Reza Ganjali, M., Khoobi, M., Nazmara, S., Hossein Mahvi, A., 2016. Modeling of Reactive Blue 19 azo dye removal from colored textile wastewater using L-arginine-functionalized Fe_3O_4 nanoparticles: Optimization, reusability, kinetic and equilibrium studies. J. Magnet. Magnetic Mater. 404, 179–189.

de Jesus, C. P. C., Antunes, M. L. P., da Conceição, F. T., Navarro, G. R. B., Moruzzi, R. B., 2015. Removal of reactive dye from aqueous solution using thermally treated red mud. Desalin. Water Treat. 55, 1040–1047.

de Souza, K.C., Antunes, M.L.P., Couperthwaite, S.J., da Conceição, F.T., de Barros, T.R., Frost, R., 2013. Adsorption of reactive dye on seawater-neutralized bauxite refinery residue. J. Colloid Interf. Sci. 396, 210–214.

Debrassi, A., Baccarin, T., Demarchi, C. A., Nedelko, N., Ślawska-Waniewska, A., Dluzewski, P., Bilska, M., Rodrigues, C.A., 2012. Adsorption of Remazol Red 198 onto magnetic N-lauryl chitosan particles: Equilibrium, kinetics, reuse and factorial design. Environ. Sci. Pollution Res. 19, 1594–1604.

Demarchi, C. A., Debrassi, A., de Campos Buzzi, F., Nedelko, N., Ślawska-Waniewska, A., Dłuzewski, P., Dal Magro, J., Scapinello, J., Rodrigues, C.A., 2015. Adsorption of the dye Remazol Red 198 (RR198) by O-carboxymethylchitosan-N-lauryl/γ-Fe_2O_3 magnetic nanoparticles. Arab. J. Chem. 8. DOI: 10.1016/j.arabjc.2015.08.028

Dhanapal, V., Subramanian, K., 2014. Recycling of textile dye using double network polymer from sodium alginate and superabsorbent polymer. Carbohyd. Polym. 108, 65–74.

Dharajiya, D., Shah, M., Bajpai, B., 2016. Decolorization of simulated textile effluent by *Phanerochaete chrysosporium* and *Aspergillus fumigatus* A23. Nature Environ. Pollut. Technol. 15, 825–832.

Dubinin, M.M., Radushkevich, L.V., 1947. The equation of the characteristic curve of the activated charcoal. Proc. Acad. Sci. USSR Phys. Chem. Sect. 55, 331–337.

Duman, O., Tunç, S., Bozoğlan, B. K., Polat, T.G., 2016. Removal of triphenylmethane and reactive azo dyes from aqueous solution by magnetic carbon nanotube-κ-carrageenan-Fe_3O_4 nanocomposite. J. Alloys Comp. 687, 370–383.

El-Naggar, M.E., Radwan, E.K., El-Wakeel, S.T., Kafafy, H., Gad-Allah, T.A., El-Kalliny, A.S., Shaheen, T.I., 2018. Synthesis, characterization and adsorption properties of

microcrystalline cellulose-based nanogel for dyes and heavy metals removal. Int. J. Biologic. Macromol. 113, 248-258.

Elwakeel, K.Z., 2009. Removal of Reactive Black 5 from aqueous solutions using magnetic chitosan resins. J. Hazard. Mater. 167, 383–392.

Errais, E., Duplaya, J., Elhabiri, M., Khodjac, M., Ocampod, R., Baltenweck-Guyote, R., Darragi, F., 2012. Anionic RR120 dye adsorption onto raw clay: surface properties and adsorption mechanism. Colloids Surf. A, 403, 69–78

Ferrero, F., 2007. Dye removal by low-cost adsorbents: hazelnut shells in comparison with wood sawdust. J. Hazard. Mater. 142, 144–52.

Fettouche, S., Tahiri, M., Madhouni, R., Cherkaoui, O., 2015. Removal of reactive dyes from aqueous solution by adsorption onto Alfa fibers powder. J. Mater. Environ. Sci. 6, 129–137.

Figueiredo, S.A., Boaventura, R.A., Loureiro, J.M., 2000. Color removal with natural adsorbents: Modelling, simulation and experimental. Separat. Purific. Technol. 20, 129–141.

Filipkowska, U. Adsorption and desorption of reactive dyes onto chitin and chitosan flakes and beads. Adsorp. Sci. Technol. 2006, 24, 781–795.

Fontana, J.D., Baldo, G.R., Grzybowski, A., Tiboni, M., Scremin, L.B., Koop, H.S., Santana, M.J., Lião, L.M., Döhler, L., 2016. Textile cotton dust waste: partial diethylamino-ethylation and its application to the sorption/removal of the model residual textile dye Reactive Red 239. Polym. Bull. 73, 3401–3420.

Freundlich, H.M.F. Over the adsorption in solution. J. Phys. Chem. 1906, 57, 385–471.

Gao, J., Si, C., He, Y., 2015. Application of soybean residue (okara) as a low-cost adsorbent for reactive dye removal from aqueous solution. Desalin. Water Treat. 53, 2266–2277.

Ghaneian, M.T., Jamshidi, B., Dehvari, M., Amrollahi, M., 2015. Pomegranate seed powder as a new biosorbent of reactive red 198 dye from aqueous solutions: Adsorption equilibrium and kinetic studies. Res. Chem. Intermed. 41, 3223–3234.

Gingell, R., Walker, R., 1971. Mechanisms of azo reduction by Streptococcus faecalis. II. The role of soluble flavins. Xenobiotica 1, 231–9.

Guendouz, S., Khellaf, N., Djelal, H., Ouchefoun, M., 2016. Simultaneous biosorption of the two synthetic dyes, Direct Red 89 and Reactive Green 12 using nonliving macrophyte L. gibba L. Desalin. Water Treat. 57, 4624–4632.

Gül, Ü. D., Dönmez, G., 2013. Application of mixed fungal biomass for effective reactive dye removal from textile effluents. Desalin. Water Treat. 51, 3597–3603.

Gunay, A., Arslankaya, E., Tosun, I., 2007. Lead removal from aqueous solution by natural and pre-treated clinoptilolite: adsorption equilibrium and kinetics. J. Hazard. Mater. 146, 362–371.

Hassan, M.M., 2014. Enhanced antistatic and mechanical properties of corona plasma-treated wool fabrics treated with 2,3-epoxypropyltrimethylammonium chloride. Ind. Eng. Chem. Res. 53, 10954–10964.

Hassan, M.M., 2015. Binding of a quaternary ammonium polymer-grafted-chitosan onto a chemically modified wool fabric surface: Assessment of mechanical, antibacterial and antifungal properties. RSC Adv. 5, 35497–35505.

Ho, Y.S., 2004. Citation review of Lagergren kinetic rate equation on adsorption reactions. Scientometrics 59, 171–177.

Ho, Y.S., Wase, D.A.J., Forster, C.F., 1996. Removal of lead ions from aqueous solution using sphagnum moss peat as adsorbent. Water SA 22, 219–224.

Honorio, J.F., Veit, M.T., Da Cunha Gonçalves, G., De Campos, E.A., Fagundes-Klen, M.R., 2016. Adsorption of reactive blue BF-5G dye by soybean hulls: Kinetics, equilibrium and influencing factors. Water Sci. Technol. 73, 1166–1174.

Hu, T.L., 1996. Removal of reactive dyes from aqueous solution by different bacterial genera. Water Sci. Technol. 34, 89–95.

Ignat, M.-E., Dulman, V., Onofrei, T., 2012. Reactive Red 3 and Direct Brown 95 dyes adsorption onto chitosan. Cellulose Chem. Technol. 46, 357–367.

Iscen, C.F., Kiran, I., Ilhan, S., 2007. Biosorption of Reactive Black 5 dye by *Penicillium restrictum*: The kinetic study. J. Hazard. Mater. 143, 335–340.

Jafari, A.J., Kakavandi, B., Kalantary, R.R., Gharibi, H., Asadi, A., Azari, A., Babaei, A.A., Takdastan, A., 2016. Application of mesoporous magnetic carbon composite for reactive dyes removal: Process optimization using response surface methodology. Korean J. Chem. Eng. 33, 2878–2890.

Janaki, V., Vijayaraghavan, K., Oh, B.-T., Lee, K.-J., Muthuchelian, K., Ramasamy, A.K., Kamala-Kannan, S., 2012. Starch/polyaniline nanocomposite for enhanced removal of reactive dyes from synthetic effluent. Carbohyd. Polym. 90, 1437–1444.

Jiang, X., Sun, Y., Liu, L., Wang, S., Tian, X., 2014. Adsorption of C.I. Reactive Blue 19 from aqueous solutions by porous particles of the grafted chitosan. Chem. Eng. J. 235, 151–157.

Jóźwiak, T., Filipkowska, U., Szymczyk, P., Kuczajowska-Zadrożna, M., Mielcarek, A., 2015. Application of chitosan ionically cross-linked with sodium edetate for reactive dyes removal from aqueous solutions. Prog. Chem. Applicat. Chitin Derivat. 20, 82–96.

Kadam, A.A., Lee, D.S., 2015. Glutaraldehyde cross-linked magnetic chitosan nanocomposites: Reduction precipitation synthesis, characterization, and application for removal of hazardous textile dyes. Bioresour. Technol. 193, 563–567.

Kalkan, E., Nadaroğlu, H., Celebi, N., Tozsin, G., 2014. Removal of textile dye Reactive Black 5 from aqueous solution by adsorption on laccase-modified silica fume. Desalin. Water Treat. 52, 6122–6134.

Kannusamy, P., Sivalingam, T., 2013. Synthesis of porous chitosan-polyaniline/ZnO hybrid composite and application for removal of reactive orange 16 dye. Colloid. Surf. B: Biointerf. 108, 229–238.

Kara, I., Akar, S. T., Akar, T., Ozcan, A., 2012. Dithiocarbamated *Symphoricarpus albus* as a potential biosorbent for a reactive dye. Chem. Eng. J. 211–212, 442–452.

Karcher, S., Kornmuller, A., Jekel, M., 2002. Anion exchange resins for removal of reactive dyes from textile wastewaters. Water Res. 36, 4717–4724.

Karim, M.E., Dhar, K., Hossain, M.T., 2017. Co-metabolic decolorization of a textile reactive dye by Aspergillus fumigatus. Int. J. Environ. Sci. Technol. 14, 177–186.

Khoshhesab, Z. M., Gonbadi, K., Rezaei Behbehani, G., 2015. Removal of reactive black 8 dye from aqueous solutions using zinc oxide nanoparticles: Investigation of adsorption parameters. Desalin. Water Treat. 56, 1558–1565.

Kim, S., Won, S.W., Cho, C.-W., Yun, Y.-S., 2016. Valorization of Escherichia coli waste biomass as a biosorbent for removing reactive dyes from aqueous solutions. Desalin. Water Treat. 57, 20084–20090.

Kim, S.-Y., 2007. Improvement of the decolorization of azo dye by anaerobic sludge bioaugmented with *Desulfovibrio desulfuricans*. Biotechnol. Bioproc. Eng. 12, 222–227.

Kim, T.-Y., Park, S.-S., Cho, S.-Y., 2012. Adsorption characteristics of Reactive Black5 onto chitosan beads cross-linked with epichlorohydrin. J. Ind. Eng. Chem. 18, 1458–1464.

Kumari K., Abraham T.E., 2007. Biosorption of anionic textile dyes by nonviable biomass of fungi and yeast. Bioresour. Technol. 98, 1704–10.

Kyzas, G.Z., Fu, J., Matis, K.A., 2013. The Change from past to future for adsorbent materials in treatment of dyeing wastewaters. Materials 6, 5131–5158.

Kyzas, G.Z., Lazaridis, N.K., 2009. Reactive and basic dyes removal by sorption onto chitosan derivatives. J. Colloid Interf. Sci. 331, 32–39.

Lambert, S J., Davy, A.J., 2011. Water quality as a threat to aquatic plants: discriminating

Langmuir, I., 1916. The constitution and fundamental properties of solids and liquids. J. Am. Chem. Soc. 38, 2221–2295.

Li, Z., Cao, M., Zhang, W., Liu, L., Wang, J., Ge, W., Yuan, Y., Yue, T., Li, R., Yu, W.W., 2014. Affinity adsorption of lysozyme with Reactive Red 120 modified magnetic chitosan microspheres. Food Chem. 145, 749–755.

Lima, E. C., Royer, B., Vaghetti, J. C. P., Simon, N. M., da Cunha, B. M., Pavan, F. A., Benvenutti, E.V., Veses, R.C., Airoldi, C., 2008. Application of Brazilian-pine fruit coat as a biosorbent to removal of reactive red 194 textile dye from aqueous solution, Kinetics and equilibrium study. J. Hazard. Mater. 155, 536–550.

Low, K.S., Lee, C.K., 1997. Quaternized rice husk as sorbent for reactive dyes. Bioresour. Technol. 61, 121–125.

Low, K.-S., Lee, C.-K., Tan, B.-F., 2000. Quaternized wood as sorbent for reactive dyes. Appl. Biochem. Biotechnol. A: Enzyme Eng. Biotechnol. 87, 233–245.

Ma, Q., Wang, L., 2015. Adsorption of Reactive blue 21 onto functionalized cellulose under ultrasonic pretreatment: Kinetic and equilibrium study. J. Taiwan Inst. Chem. Eng. 50, 229–235.

Meehan, C., Bjourson, A.J., McMullan, G., 2001. *Paenibacillus azoreducens sp. no*v., a synthetic azo dye decolorizing bacterium from industrial wastewater. Int. J. System. Evolution. Microbiol. 51, 1681–1685.

Mona, S., Kaushik, A., Kaushik, C.P., 2011. Waste biomass of Nostoc linckia as adsorbent of crystal violet dye: Optimization based on statistical model. Int. Biodeterior. Biodegrad. 65, 513–521.

Morais, L.C., Freitas, O.M., Goncalves, E.P., Vasconcelos, L.T., Gonzalez Beca, C.G., 1999. Reactive dyes removal from wastewaters by adsorption on Eucalyptus bark: variables that define the process. Water Res. 33, 979–988.

Nadafi, K., Vosoughi, M., Asadi, A., Borna, M. O., Shirmardi, M., 2014. Reactive Red 120 dye removal from aqueous solution by adsorption on nano-alumina. J. Water Chem. Technol. 36, 125–133.

Ncibi, M. C., Mahjoub, B., Seffen, M. Adsorptive removal of textile reactive dye using Posidonia oceanic (L) fibrous biomass. Int. J. Environ. Sci. Technol. 2007, 4, 433–440.

Nga, N.K., Chinh, H.D., Hong, P.T.T., Huy, T.Q., 2017. Facile preparation of chitosan films for high-performance removal of Reactive Blue 19 dye from aqueous solution. J. Polym. Environ. 25, 146–155.

Ovando-Medina, V. M., Vizcaíno-Mercado, J., González-Ortega, O., De La Garza, J. A. R., Martínez-Gutiérrez, H., 2015. Synthesis of α-cellulose/polypyrrole composite for the removal of reactive red dye from aqueous solution: Kinetics and equilibrium modeling. Polym. Compos. 36, 312–321.

Oxspring, D.A., McMullan, G., Smyth, W.F., Marchant, R., 1996. Decolorization and metabolism of the reactive textile dye, Remazol Black B, by an immobilized microbial consortium. Biotechnol. Lett. 18, 527–30.

Patle, D.B., Gurnule, W.B., 2016. An eco-friendly synthesis, characterization, morphology and ion exchange properties of terpolymer resin derived from *p*-hydroxybenzaldehyde. Arab. J. Chem. 9, S648-S658.

Pearce, C.I., Lloyd, J.R., Guthrie, J.T., 2003. The removal of color from textile wastewater using whole bacterial cells: A review. Dyes Pigment. 58, 179–196.

Plumb, J.J., Bell, J., Stuckey, D.C., 2001. Microbial populations associated with treatment of an industrial dye effluent in an anaerobic baffled reactor. Appl. Environ. Microbiol. 67, 3226–35.

Rahman, A., Urabe, T., Kishimoto, N., 2013. Color removal of Prion reactive dyes by clay adsorbents. Procedia Environ. Sci. 17, 270–278.

Ram, N., 2017. China Dyes & Pigment Industry in FY 2016 - An Overview, https://www.linkedin.com/pulse/china-dyes-pigment-industry-fy-2016-overview-ram-n (accessed on 25 May, 2017).

Ratnamala, G. M., Deshannavar, U. B., Munyal, S., Tashildar, K., Patil S., Shinde, A., 2016. Adsorption of reactive blue dye from aqueous solutions using sawdust as adsorbent: Optimization, kinetic, and equilibrium studies. Arabian J. Sci. Eng. 41, 333–344.

Reddy, M.C.S, Nirmala, V., Ashwini, C., 2017. Bengal Gram Seed Husk as an adsorbent for the removal of dye from aqueous solutions – Batch studies. Arab. J. Chem. 10, 2554–S2566.

Redlich, O., Peterson, D.L., 1959. A useful adsorption isotherm. J. Phys. Chem. 63, 1024–1026.

Robinson, T., McMullan, G., Marchant, R., Nigam, P., 2001. Remediation of dyes in textile effluent: A critical review on current treatment technologies with a proposed alternative. Bioresour. Technol. 77, 247–55.

Rosa, S., Laranjeira, M.C.M., Riela, H.G., Fávere, V.T., 2008. Cross-linked quaternary chitosan as an adsorbent for the removal of the reactive dye from aqueous solutions. J. Hazard. Mater. 155, 253–260.

Saeed, M., Nadeem, R., Yousaf, M., 2015. Removal of industrial pollutant (Reactive Orange 122 dye) using environment-friendly sorbent *Trapa bispinosa*'s peel and fruit. Int. J. Environ. Sci. Technol. 12, 1223–1234.

Samarghandi, M.R., Hadi, M., Moayedi, S., Askari, F.B., 2009. Two-parameter isotherms of methyl orange sorption by pinecone derived activated carbon. Iranian J. Environ. Health Sci. Eng. 6, 285–294.

San Keskin, N.O., Celebioglu, A., Sarioglu, O.F., Ozkan, A.D., Uyar, T., Tekinay, T., 2015. Removal of a reactive dye and hexavalent chromium by a reusable bacteria attached electrospun nanofibrous web. RSC Adv. 5, 86867–86874.

Shuang, C., Li, P., Li, A., Zhou, Q., Zhang, M., Zhou, Y., 2012. Quaternized magnetic microspheres for the efficient removal of reactive dyes. Water Res. 46, 4417–4426.

Sinha, A., Osborne, W.J., 2016. Biodegradation of reactive green dye (RGD) by indigenous fungal strain VITAF-1. Int. Biodeterior. Biodegrad. 114, 176–183.

Sips, R., 1948. Combined form of Langmuir and Freundlich equations. J. Chem. Phys. 16, 490–495.

Song, K., Xu, H., Xu, L., Xie, K., Yang, Y., 2017. Cellulose nanocrystal-reinforced keratin bioadsorbent for effective removal of dyes from aqueous solution. Bioresour. Technol. 232, 254–262.

Subramani, S.E., Thinakaran, N., 2017. Isotherm, kinetic and thermodynamic studies on the adsorption behavior of textile dyes onto chitosan. Process Safety Environ. Protec. 106, 1–10.

Sumari, S. M., Hamzah, Z., Kantasamy, N., 2016. Adsorption of anionic dyes from aqueous solutions by calcined and uncalcined Mg/Al layered double hydroxide. Malaysian J. Anal. Sci. 20, 777–792.

Sun, D., Zhang, Z., Wang, M., Wu, Y., 2013. Adsorption of reactive dyes on activated carbon developed from Enteromorpha prolifera. Am. J. Analyt. Chem. 4, 17–26.

Suteu, D., Zaharia, C., Malutan, T., 2011. Removal of Orange 16 reactive dye from aqueous solutions by waste sunflower seed shells. J. Serb. Chem. Soc. 76, 607–624.

Suteu, D., Malutan, T., Bilba, D., 2010. Removal of reactive dye Brilliant Red HE-3B from aqueous solutions by industrial lignin: Equilibrium and kinetics modeling. Desalination 255, 84–90.

Tanyildizi, M.S., 2011. Modeling of adsorption isotherms and kinetics of reactive dye from aqueous solution by peanut hull. Chem. Eng. J. 168, 1234–1240.

Thangamani, K.S., Sathishkumar, M., Sameena, Y., Vennilamani, N., Kadirvelu, K., Pattabhi, S., Yun, S.E., 2007. Utilization of modified silk cotton hull waste as an adsorbent for the removal of textile dye (Reactive Blue MR) from aqueous solution. Bioresour. Technol. 98, 1265–1269.

Toth, J., 1971. State equations of the solid-gas interface layer. Acta Chem. Acad. Hung. 69, 311–317.

Vakili, M., Rafatullah, M., Salamatinia, B., Ibrahim, M.H., Abdullah, A.Z., 2015. Elimination of reactive blue 4 from aqueous solutions using 3-aminopropyl triethoxysilane modified chitosan beads. Carbohyd. Polym. 132, 89–96.

Venkatesha, T.G., Viswanatha, R., Arthoba Nayaka, Y., Chethana, B.K., 2012. Kinetics and thermodynamics of reactive and vat dyes adsorption on MgO nanoparticles. Chem. Eng. J. 198–199, 1–10.

Vijayaraghavan, K., Padmesh, T.V.N., Palanivelu, K., Velan, M., 2006. Biosorption of nickel(II) ions onto Sargassum *wightii*: application of two-parameter and three parameter isotherm models. J. Hazard. Mater. B133, 304–308.

Vijayaraghavan, K., Yun, Y.S., 2007. Utilization of fermentation waste (*Corynebacterium glutamicum*) for biosorption of Reactive Black 5 from aqueous solution. J. Hazard. Mater. 141, 45–52.

Vorotyntsev, A.V., Petukhov, A.N., Makarov, D.A., Razov, E.N., Vorotyntsev, I.V., Nyuchev, A.V., Kirillova, N.I., Vorotyntsev, V.M., 2018. Synthesis, properties and mechanism of the ion exchange resins based on 2-methyl-5-vinylpyridine and divinylbenzene in the catalytic disproportionation of trichlorosilane. Appl. Catal. B 224, 621–633.

Wang, P., Ma, Q., Hu, D., Wang, L., 2015. Removal of Reactive Blue 21 onto magnetic chitosan microparticles functionalized with polyamidoamine dendrimers. React. Function. Polym. 91–92, 43–50.

Wang, Q., Luan, Z., Wei, N., Li, J., Liu, C., 2009. The color removal of dye wastewater by magnesium chloride/red mud (MRM) from aqueous solution. J. Hazard. Mater. 170, 690–698.

Won, S.W., Kim, H.J., Choi, S.H., Chung, B.W., Kim, K.J., Yun, Y.S., 2006. Performance, kinetics and equilibrium in biosorption of anionic dye Reactive Black 5 by the waste biomass of Corynebacterium glutamicum as a low-cost biosorbent. Chem. Eng. J. 121, 37–43.

Won, S.W., Yun, Y.S., 2008. Biosorptive removal of Reactive Yellow 2 using waste biomass from lysine fermentation process. Dyes Pigm. 76, 502–507.

Wong, S.Y., Tan, Y.P., Abdullah, A.H., Ong, S.T., 2009. The removal of basic and reactive dyes using quaternized sugarcane bagasse. J. Phys. Sci. 20, 59–74.

Xie, X., Li, X., Luo, H., Lu, H., Chen, F., Li, W., 2016. The adsorption of reactive blue 19 dye onto cucurbit[8]uril and cucurbit[6]uril: An experimental and theoretical study. J. Phys. Chem. B 120, 4131–4142.

Xu, H., Zhang, Y., Jiang, Q., Reddy, N., Yang, Y., 2013. Biodegradable hollow zein nanoparticles for removal of reactive dyes from wastewater. J. Environ. Manag. 125, 33–40.

Xue, A., Zhou, S., Zhao, Y., Lu, X., Han, P., 2010. Adsorption of reactive dyes from aqueous solution by silylated palygorskite. Appl. Clay Sci. 48, 638–640.

Yagub, M.T., Sen, T.K., Afroze, S., Ang, H.M., 2014. Dye and its removal from aqueous solution by adsorption: A review. Adv. Colloids Interf. Sci. 209, 172–184.

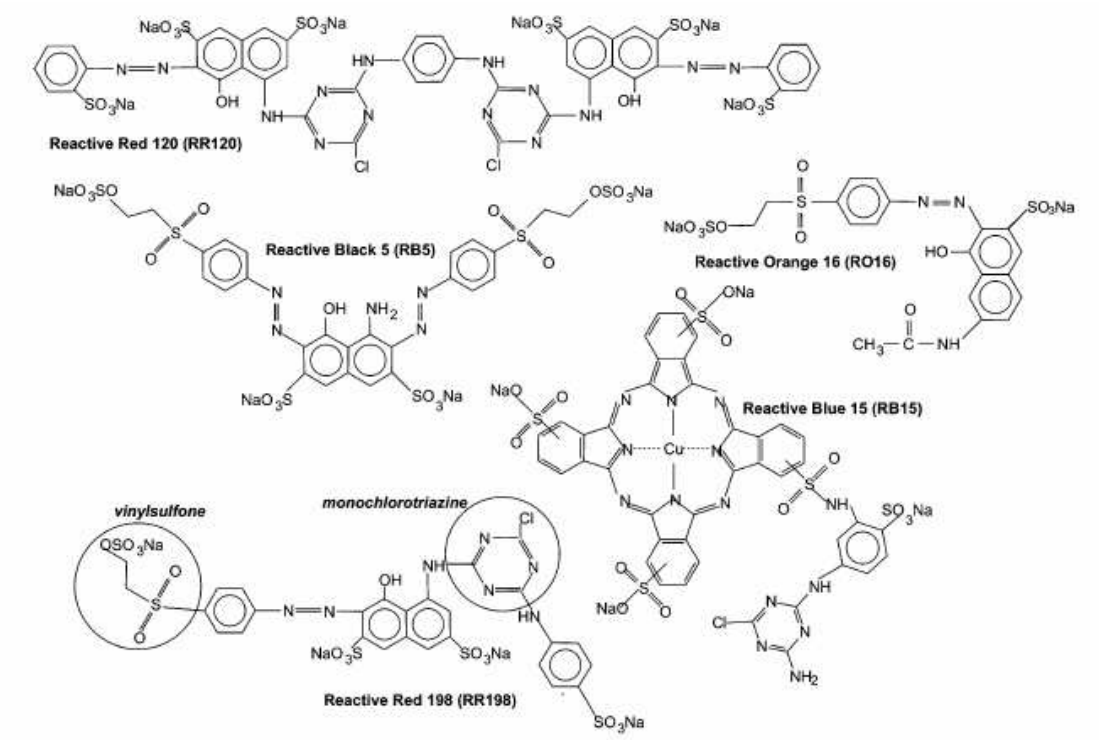

Fig. 1. Chemical structure of some common reactive dyes used for the decolourisation studies (Karcher et al., 2002).

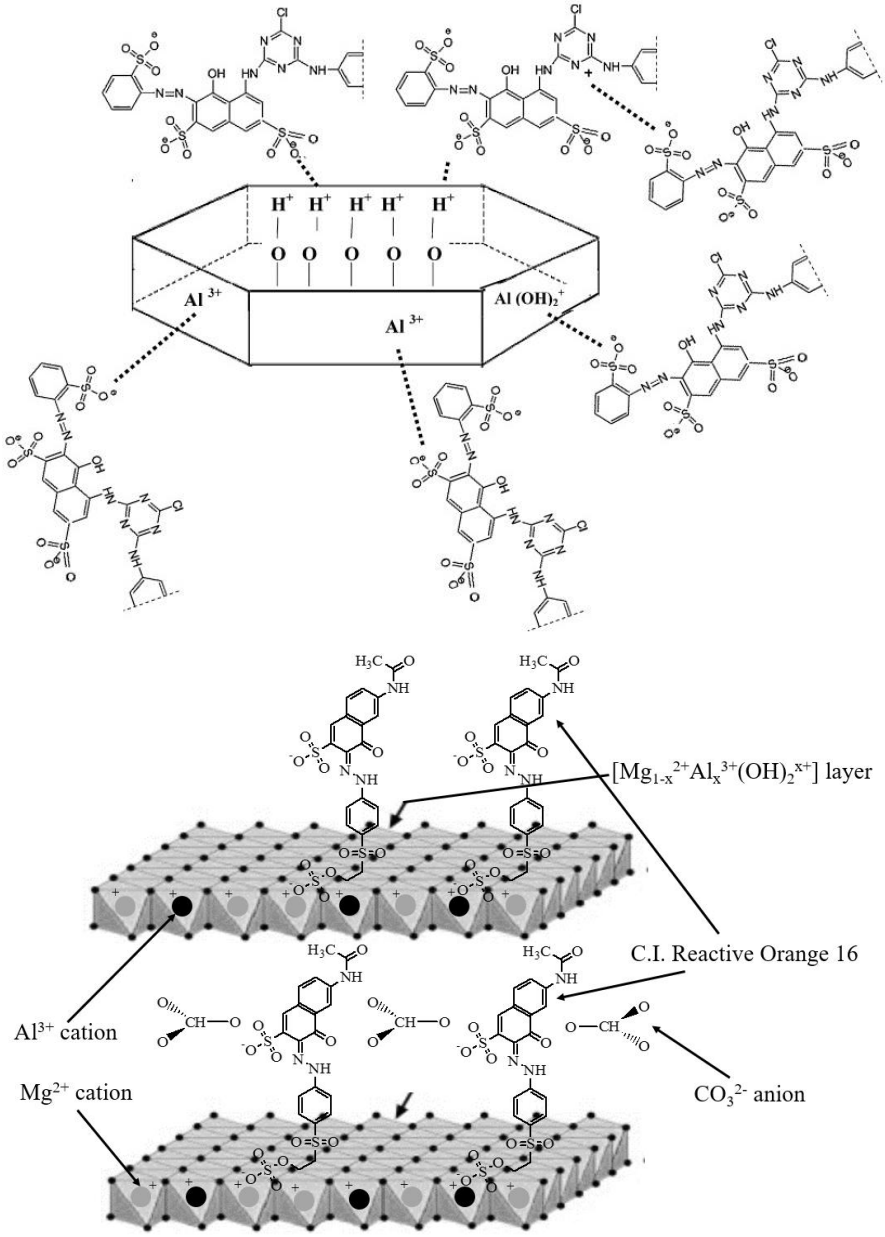

Fig. 2. Adsorption mechanisms of C.I. Reactive Red 120 and C.I. Reactive Orange 16 dye molecules onto kaolinite clay sheets (top) and Mg/Al layered double hydroxides (bottom) respectively (Khoshhesab et al., 2015).

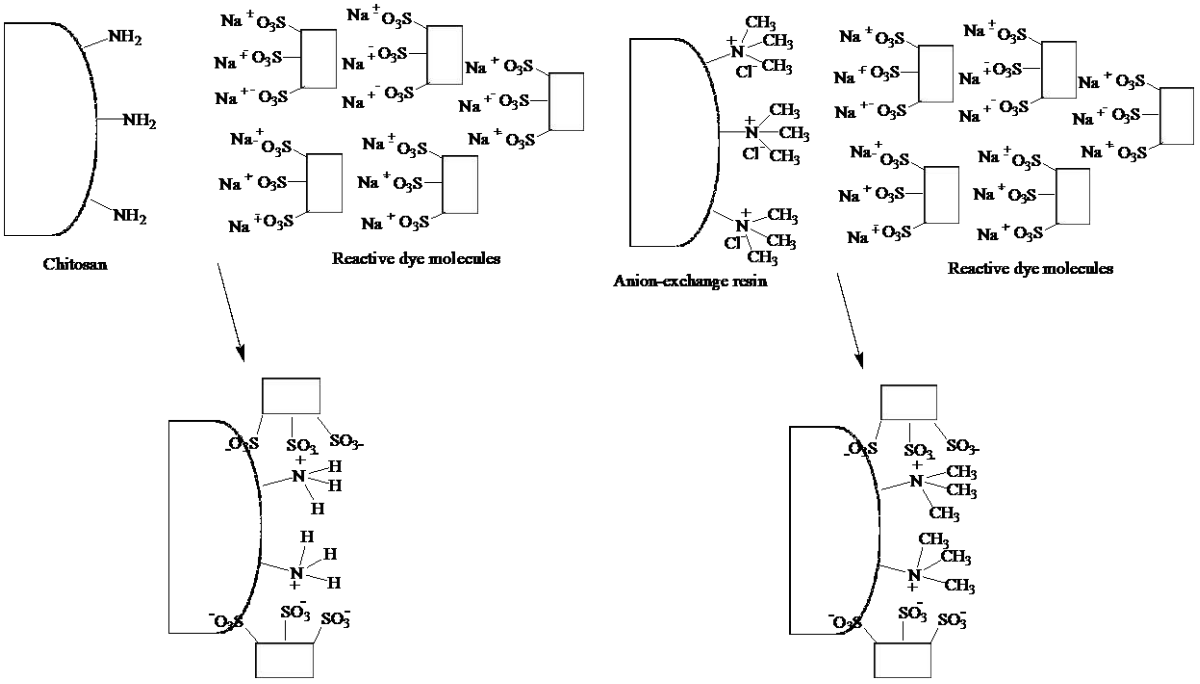

Fig. 3. Reactive Dye binding mechanism of chitosan (left) and anion-exchange resin (right).

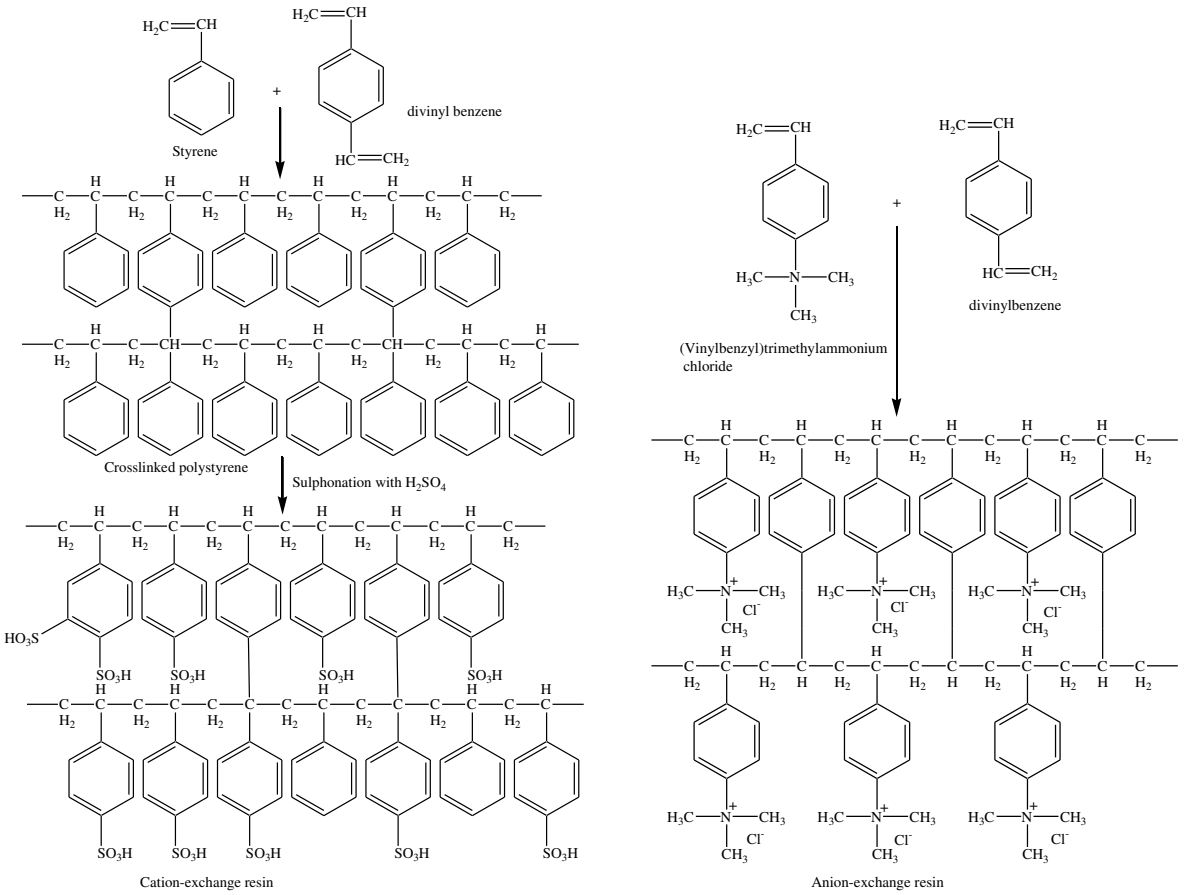

Fig. 4. Synthesis of cation-exchange and anion-exchange resins from styrene (a) and (vinylbenzyl)ammonium chloride (b) respectively by free-radical polymerisation method.

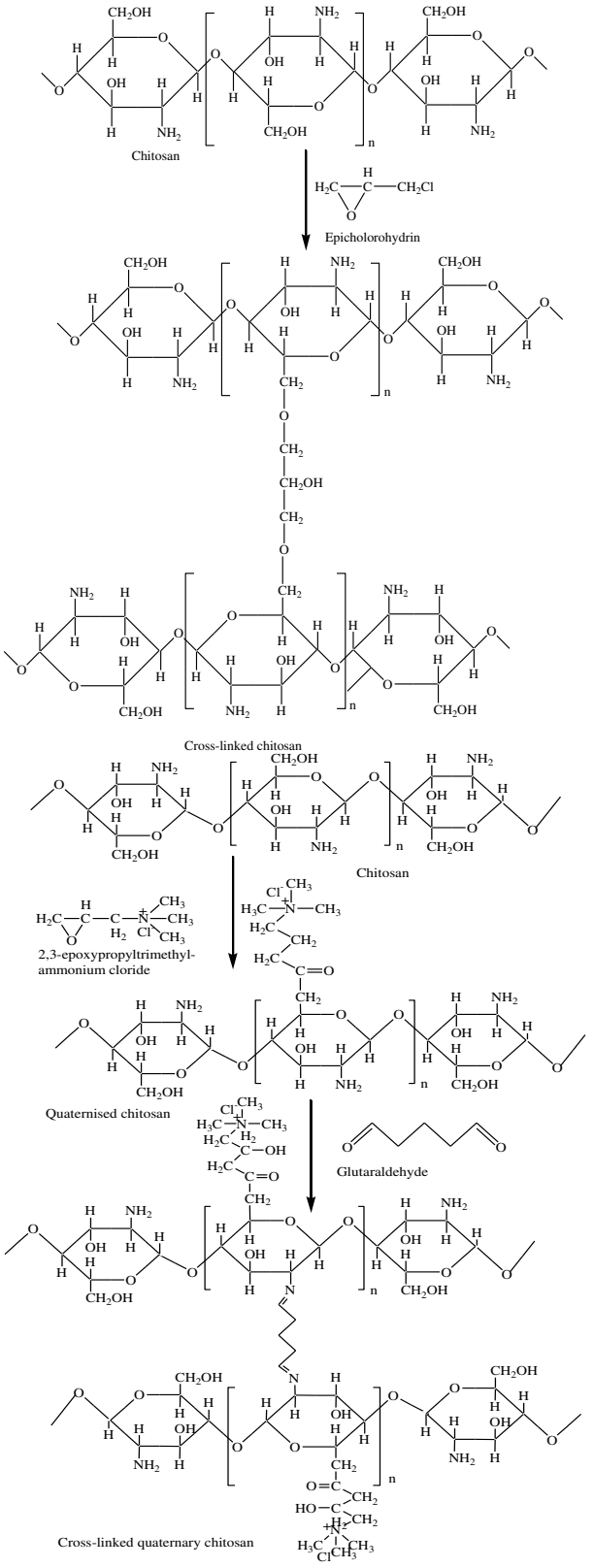
Chitosan
Epicholorohydrin
Cross-linked chitosan
Chitosan
2,3-epoxypropyltrimethyl-
ammonium cloride
Quaternised chitosan
Glutaraldehyde
Cross-linked quaternary chitosan

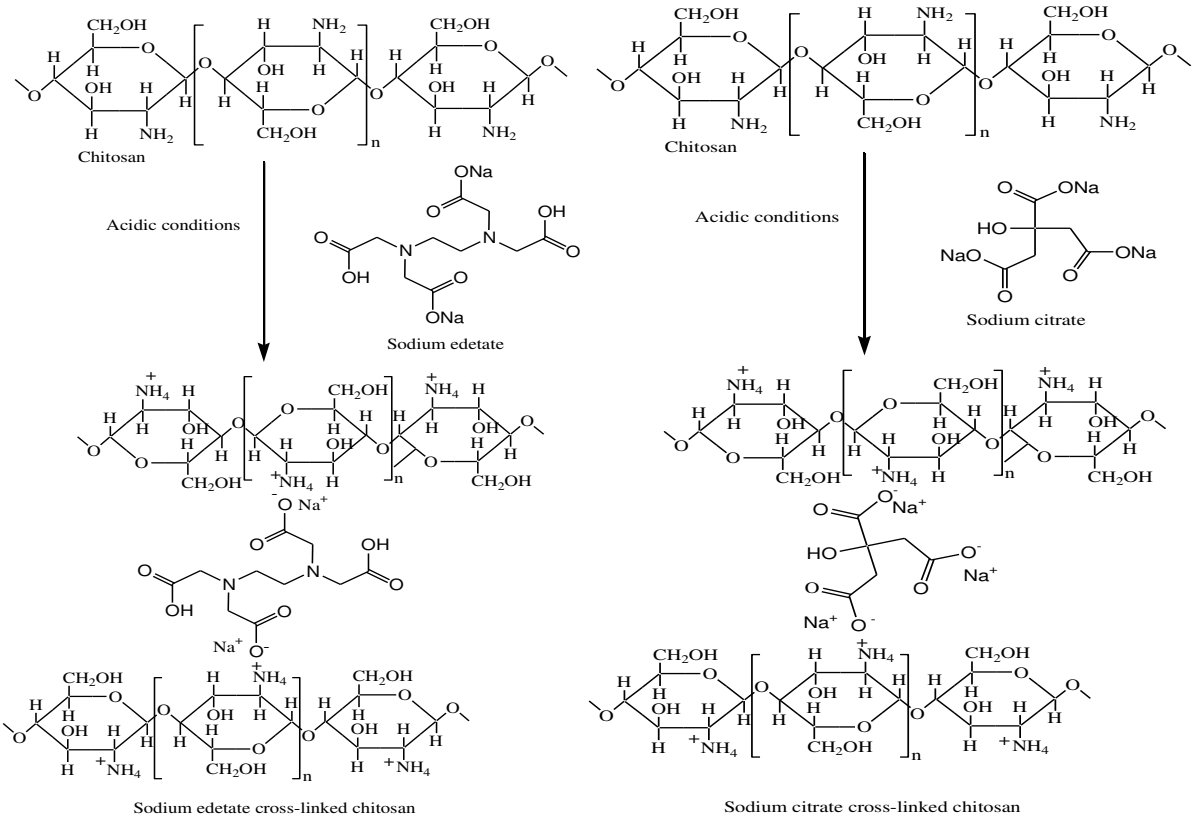

Fig. 5. Formation mechanism of chitosan adsorbents by ionic cross-linking (top) as well as by covalent bond forming cross-linking.

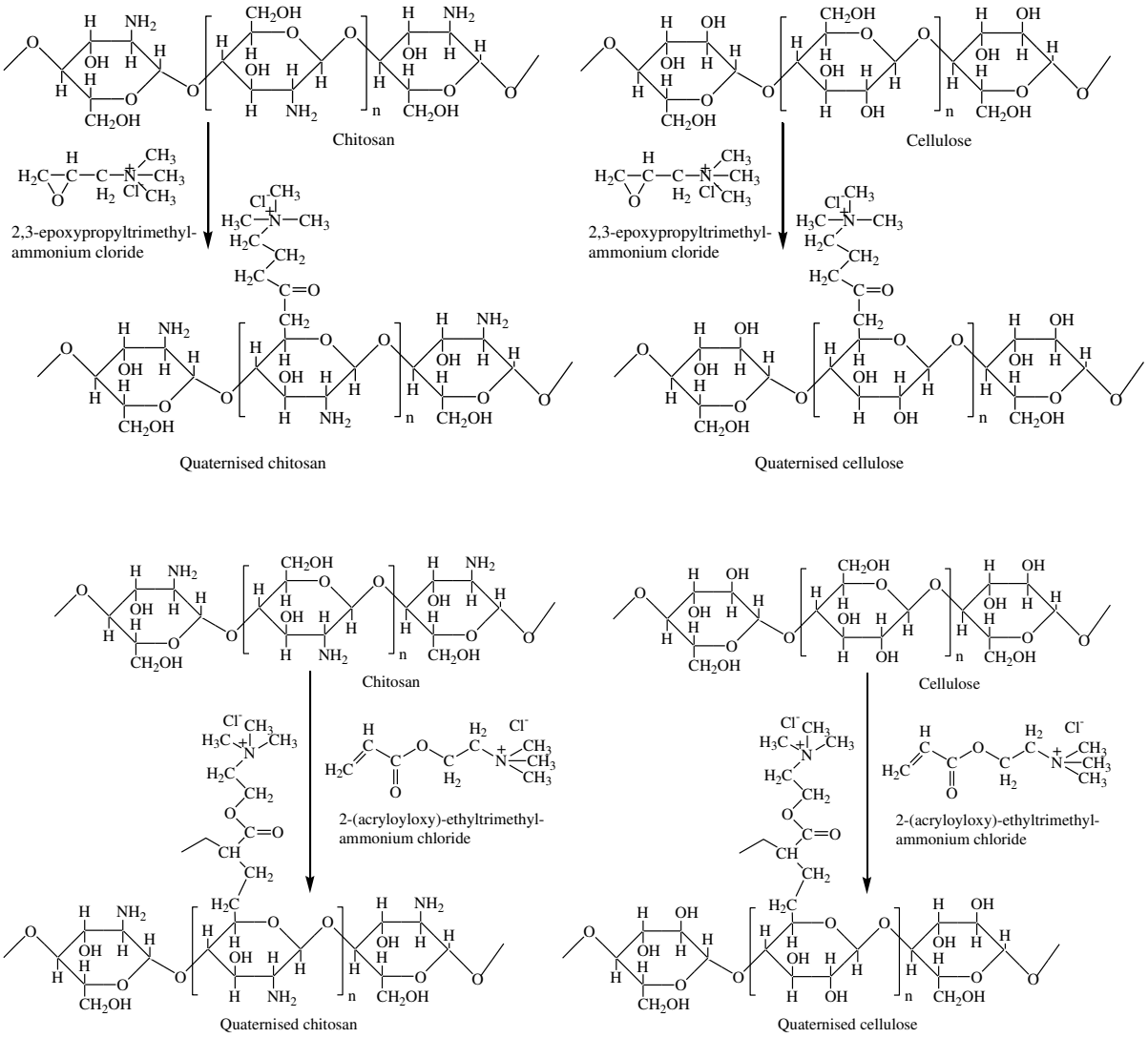

Fig. 6. Formation of quaternised chitosan and cellulose adsorbents by chemical modification with an epoxy group-containing quaternary ammonium compound (top) and by graft-copolymerisation with 2-(acryloyloxy)ethyltrimethylammonium chloride (Hassan, 2015; Hassan, 2014).

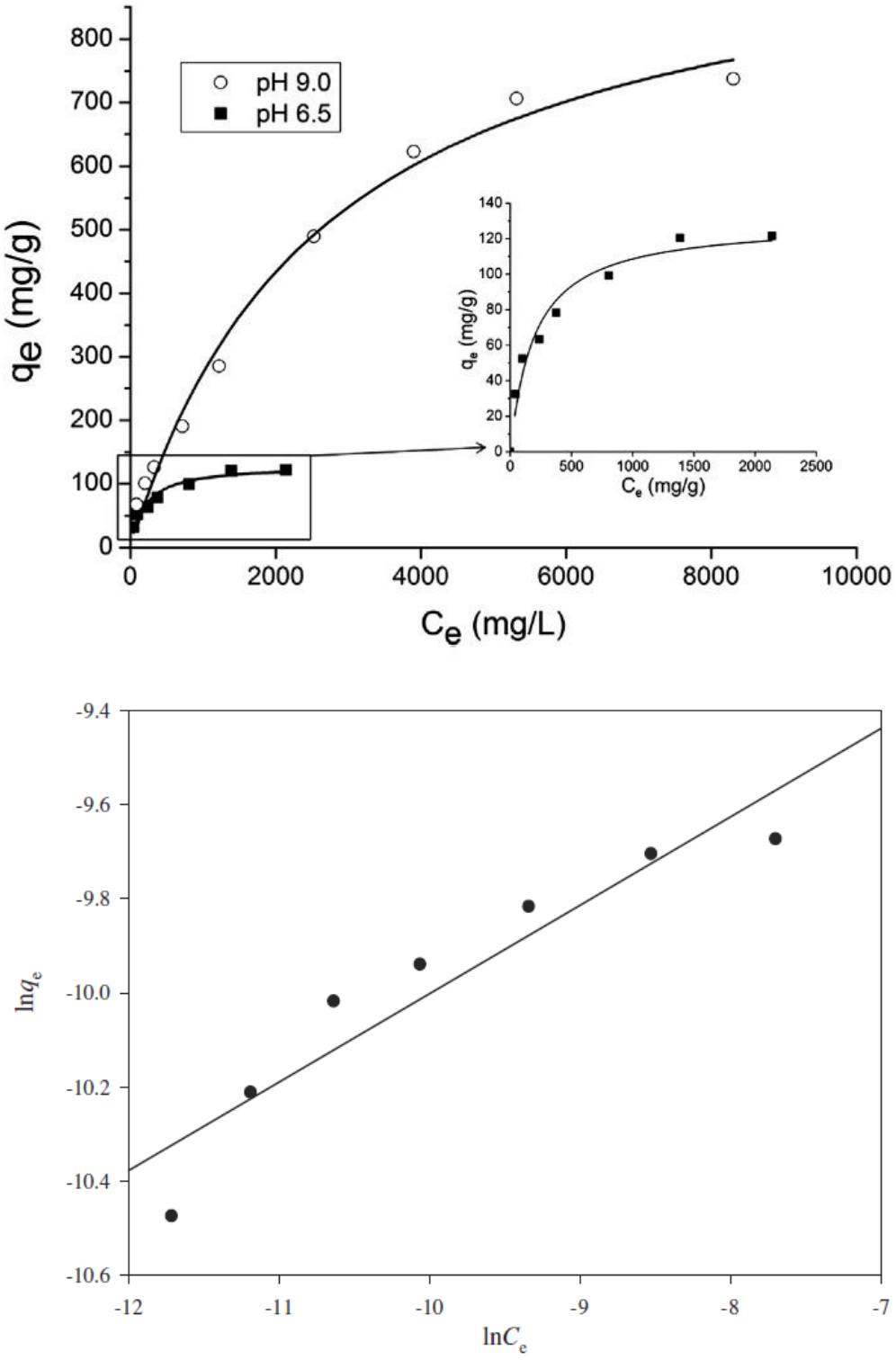

Fig. 7. Langmuir and Freundlich isotherm plots for the biosorption of C.I. Reactive Blue 19 onto hollow zein nanoparticles (top) and C.I. Reactive Red 45 onto *S. albus* (bottom) respectively [Xu et al., 2013; Kara et al., 2012].

Table 1

Annual production data (metric tons) of various dyestuffs in India from 2011-2016 (Annual report 2016-17, 2017].

Name of dyes	2011-2012	2012-2013	2013-2014	2014-2015	2015-2016
Disperse	29440	28260	29210	29560	43570
Reactive	83380	87600	95420	89470	106120
Acid	19000	17580	19000	17230	20570
Optical brightener	14140	18170	23740	22940	24700
Sulfur	7020	6580	7570	9380	9550
Vat	1690	1380	1600	1770	1440
Solubilized vat	30	30	20	30	30
Organic pigment	51770	44460	68670	76890	61310
Pigment emulsion	5220	6480	7340	9640	9670
Azoic	980	580	510	440	300
Solvent	2640	2310	2260	1800	2200

Table 2

Reactive dye binding capacity and performance of various types of ion-exchange resin adsorbents

Ion-exchange resins	Dye type	Treatment methods	Operating conditions						Dye binding capacity ($mg\ g^{-1}$)	Ref.
			Temperature of treatment (°C)	pH of maximum adsorption	Dosage of sorbent ($g\ l^{-1}$)	Agitation speed (rpm)	Dye conc. ($mg\ l^{-1}$)	Contact time (min)		
Bayer anion exchange resin (S6328a) having quarternary amine and trymethylamine groups	Reactive Black 5 Reactive Red 198	Batch	20–25	2	2	n/a	2000	4320	694.25 590.50	[Karcher et al., 2002]
Bayer anion exchange resin (MP62) having tertiary amine groups	Reactive Black 5 Reactive Red 198	Batch	20–25	2	2	n/a	2000	4320	1190.14 n/a	[Karcher et al., 2002]
SR Amberlite IRC-718 anion exchange resin	Reactive Blue 2 Reactive Orange 16 Reactive Yellow 2	Batch	23±2	n/a	5	150	500	240	1.26 3.86 3.66	[Low and Lee, 1997]
Quaternised rice husks	Reactive Blue 2 Reactive Orange 16 Reactive Yellow 2	Batch	23±2	n/a	5	150	500	240	4.90 4.40 5.00	[Low and Lee, 1997]
Poly(AA-NIPAAm-TMPTA) crosslinked with sodium alginate	C.I. Reactive Blue 4	Column	30	6	100 ml dye 10 g^{-1} adsorbent	-	5000	30	446	[Dhanapal, 2014]
Partial diethylamino-ethylated cotton dust waste	C.I. Reactive Red 239	Batch	25	6.6	5	160	500	1440	86.96	[Fontana et al., 2016]
Quaternised wood	Reactive Blue 2	Batch	28±2	11	5	150	2000	360	250.00	[Low et al., 2000]
Quaternised flax cellulose with ultrasound	Reactive Blue 21	Batch	30	9	0.31	120	200	180	543.00	[Ma and Wang, 2015]
Cucurbit[8]uril	C.I. Reactive Blue 19	Batch	25	7	0.3	n/a	300	720	714.29	[Xie et al., 2016]
Cucurbit[6]uril			24						100.5	
Quaternised sugarcane bagasse	C.I. Reactive Orange 16	Batch	25	3	5	150	100	480	22.73	[Wong et al., 2009]
Ethylenediamine functionalised activated paper sludge	Reactive Blue 19	Batch	30	2	0.4	n/a	200	1440	689.97	[Auta and Hameed, 2014]
Potassium fluoride activated paper sludge	Reactive Orange 16								696.23	
Cellulose nanocrystal-reinforced keratin	Reactive Black 5	Batch	25	2	2	n/a	200	180	1250	[Song et al., 2017]
Starch/polyaniline nanocomposite	Reactive Black 5 Reactive Violet 4	Batch	25	3	0.6	150	n/a	70	811.3 578.39	[Janaki et al., 2012]
Polypyrrole-modified-α-cellulose	Reactive Red 120	Batch	25	2	3.33	n/a	1000	8640	96.1	[Ovando-Medina et al, 2015]
Hollow zein nanoparticles	C.I. Reactive Blue 19	Batch	25	2	1	n/a	75–2260.5	1440	1016.00	[Xu et al., 2013]
Lignin chemically modified with aluminium	Reactive Blue 4	Batch	25	2	2.5	n/a	340	480	73.52	[Adebayo et al., 2014]
Lignin chemically modified with manganese									55.16	
Cationic polyelectrolyte polyepicholorohydrin-dimethylamine modified bentonite	Reactive Blue 4 Reactive yellow 18	Batch	30	2	2	n/a	150	120	63.19 110..64	[Chen et al., 2011]

Table 3

Reactive dye removal performance of lignocellulosic biomasses

Ion-exchange resins	Dye type	Treatment methods	Operating conditions						Dye binding capacity ($mg\ g^{-1}$)	Ref.
			Temperature of treatment (°C)	pH of maximum adsorption	Dosage of sorbent ($g\ l^{-1}$)	Agitation speed (rpm)	Dye conc. ($mg\ l^{-1}$)	Contact time (min)		
Trapa bispinosa's peel	C.I. Reactive Orange 122	Batch	n/a	1	2	100	350	120	29.79	[Saeed et al., 2015]
Trapa bispinosa's fruit	C.I. Reactive Orange 122	Batch	n/a	1	2	100	350	120	29.51	[Saeed et al., 2015]
Grape fruit peel	C.I. Reactive Blue 19	Batch	n/a	3	3.33	180	50	45	12.53	[Abassi and Asl, 2009]
Alfa fibres powder	C.I. Reactive Red 23	Batch	22	2	30	150	100	90	34.13	[Fettouche et al., 2015]
	C.I. Reactive Blue 19								11.33	
soybean residue	C.I. Reactive Blue 19	Batch	50	2	x	x	x	x	402.58	[Gao et al., 2015]
soybean stalk	C.I. Reactive Black 5	Batch	20±1	2	15	100	150	720	9.90	[Ashori et al., 2014]
Soybean hull	C.I. Reactive Blue 25	Batch	25	2	6	100	400	1440	57.47	[Honorio et al., 2016]
Eucalyptus bark	C.I. Reactive Blue 19	Batch	18	2.5	2	70	0.5	4320	90	[Morais et al., 1999]
Acid treated Brazilian pine fruit coat,	C.I. Reactive Red 194	Batch	25	2	1-25	n/a	500	4320	51.9	[Lima et al., 2008]
Modified walnut shell	Reactive Red	Batch	40	2.5	6	180	20-1000	300	568.2	[Cao et al., 2014]
Cupuassu shell	C.I. Reactive Black 5	Batch	25	2	10	n/a	250	2880	22.9	[Cardoso et al., 2011a]
P. oceanica leaf sheaths	C.I. Reactive Red 228	Batch	60	5	20	100	100	2880	3.50	[Ncibi et al., 2007]
Aqai palm stalk powder	C.I. Reactive Black 5	Batch	25	2	1-10	n/a	300	2880	52.3	[Cardoso et al., 2011b]
	C.I. Reactive Orange 16								61.3	
Acid-treated Aqai palm stalk powder	C.I. Reactive Black 5								72.3	
	C.I. Reactive Orange 16								156	
Brazilian pine-fruit shells	C.I. Reactive Black 5	Batch	30 40 50	2	4	n/a	100	720	55.6 64.8 74.6	[Cardoso et al., 2011c]

Table 4

Absorption of reactive dyes by chitosan and chitosan derivatives

Ion-exchange resins	Dye type	Treatment methods	Operating conditions						Dye binding capacity ($mg\ g^{-1}$)	Ref.
			Temperature of treatment (°C)	pH of maximum adsorption	Dosage of sorbent ($g\ l^{-1}$)	Agitation speed (rpm)	Dye conc. ($mg\ l^{-1}$)	Contact time (min)		
Chitosan alone										
Commercial chitosan powder	Reactive Black 13	Batch	30	6.7	10	n/a	200	20	91.5	[Jiang et al., 2014]
Chitosan bead	C.I. Reactive Red 189	Batch	30	1 9	2	n/a	3768	7200	1189.0 756.0	[Chiou and Li, 2002]
Chitosan	C.I. Reactive Red 3	Batch	20		1.2	400	100	1440	81.4	[Filipkowska, 2006]
Chitosan	C.I. Reactive Black 5	Batch	25 45 65	2	1	160	300	1440	224.0 284.0 345.0	[Nga et al., 2017]
Squid pen	C.I. Reactive Green 12	Batch	20	n/a	n/a	100	180	21600	202.00	[Figueiredo et al., 2000]
Chitosan powder	C.I. Reactive Red 198	Batch	25	4	0.5	175	80	360	1250.0	[Subramani and Thinakaran, 2017]
Chitosan film	C.I. Reactive Blue 19	Batch	20	6.8	n/a	150	1000	150	799.0	[Chiou et al., 2004]
Chitosan derivatives										
Porous chitosan-polyaniline/ZnO hybrid composite	Reactive Orange 16	Batch	37±0.2	3	1	100	50	60	476.2	[Kannusamy and Sivalingam, 2013]
ECH crosslinked chitosan nanoparticles	Reactive Black 5 Reactive Orange 16	Batch	30	2	0.9	n/a	8000	9600	5572.0 5392.0	[Chen et al., 2011]
ECH crosslinked chitosan bead	C.I. Reactive Red 189	Batch	30	1	2	n/a	3768	7200	1642.0	[Chiou and Li, 2002]
ECH-crosslinked chitosan beads	Reactive Blue 2	Batch		3					2498.0	[Chiou et al., 2004]
Chitosan X-linked by sodium edetate	Reactive Black 5 Reactive Yellow 84	Batch	20 60	4	1	150	200-4000	336	1025.6 1539.7	[Jóźwiak et al., 2015]
X-linked quaternised chitosan	Reactive Orange 16	Batch	25	3	1	250	1000	2000	1060.00	[Rosa et al., 2008]
3-aminopropyl 7 triethoxysilane modified chitosan beads	Reactive Blue 4	Batch		4	1	200	500	480	317.12	[vakili et al., 2015]
Polyethyleneimine-grafted-chitosan hydrogel beads	C.I. Reactive Black 5	Batch	30	5	20	150	500	1440	709.3	[Chatterjee et al., 2011]
Polyethyleneimine-grafted-chitosan hydrogel beads with sodium dodecyl sulphate									413.2	
Epichlorohydrin-crosslinked chitosan beads	C.I. Reactive Red 222	Batch	30	3	1	100	1000	1440	2252.0	[Chiou et al., 2003]
Chitosan powder grafted with poly(acrylamide)	C.I. Reactive Yellow 176	Batch	25	2	1	n/a	100	1440	928.0	[Kyzas and Lazaridis, 2009]
Chitosan bead grafted with poly(acrylamide)									863.0	

Table 5

Removal performance of reactive dyes by magnetic nanoparticles

Adsorbents	Dye type	Treatment methods	Operating conditions						Absorption capacity ($mg\ g^{-1}$)	Ref.
			Temperature of treatment (°C)	pH of maximum adsorption	Dosage of sorbent ($g\ l^{-1}$)	Agitation speed (rpm)	Dye conc. ($mg\ l^{-1}$)	Contact time (min)		
Laccase immobilised magnetic chitosan beads	C.I. Reactive Yellow 2	Batch	30	5.5	20	n/a	50	1080	2.05	[Bayramoglu et al., 2010]
	C.I. Reactive Blue 4								1.42	
Magnetic chitosan microparticles functionalised with polyamidoamine dendrimers	C.I. Reactive Blue 21	Batch	30	6.4		120	80	720	555.56	[Wang et al., 2015]
Magnetic N-lauryl chitosan particles	C.I. Reactive Red 198	Batch	25	3	1.25	n/a	500	60	374.00	[Debrassi et al., 2012]
Quaternised GLA crosslinked chitosan/magnetite nanoparticles	C.I. Reactive Black 5	Batch	25	3	1.11	300	1938.6	180	773.60	[Elwakeel, 2009]
Magnetic chitosan nanoparticle	C.I. Reactive Blue 4	Batch		4	1	200	500	480	433.74	[Jafari et al., 2016]
Modified magnetic chitosan microspheres	Reactive red 120	Batch	25± 2	7	3	200	3333.33	120	166.7	[Li et al., 2014]
Magnetic carbon nanotube-κ-carrageenan-Fe_3O_4 nanocomposite	C.I. Reactive Black 5	Batch	25	2	0.4	150	19.84	1440	22.01	[Duman et al., 2016]
Quaternised magnetic resin microspheres	C.I. Reactive Red 120	Batch	20	5	0.2	130	669	50 h	1029.0	[Shuang et al., 2012]
	C.I. Reactive Orange 16						308.8		1173.3	
O-carboxymethyl chitosan-N-lauryl/c-Fe_2O_3 magnetic nanoparticles	C.I. Reactive Red 198	Batch	25	2	1	n/a	250	120	216	[Demarchi et al., 2015]
			55						390	
L-arginine-functionalised Fe_3O_4 nanoparticles	C.I. Reactive Blue 19	Batch	25	3	0.74	250	50	2880	66.66	[Dalvand et al., 2016]
Magnetic Fe_3O_4/chitosan nanoparticles	C.I. Reactive Red 2	Batch	25± 0.5	2	0.6	180	200	300	476.8	[Cao et al., 2014]

Graphical abstract

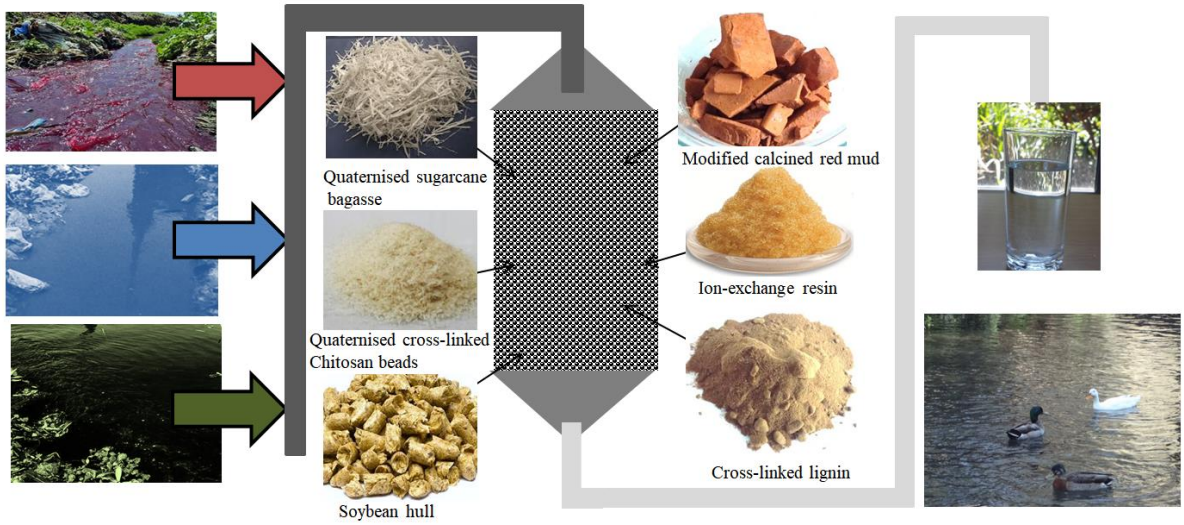

A Critical Review on Recent Advancements of the Removal of Reactive Dyes from Dyehouse Effluent by Ion-exchange Adsorbents

Mohammad M. Hassan[1], Christopher M. Carr[2]

[1] *Food & Bio-based Products Group, AgResearch Limited, Private Bag 4749, Christchurch 8140, New Zealand.*

[2] *School of Design, University of Leeds, Leeds LS2 5JQ, United Kingdom.*

Supplementary Content

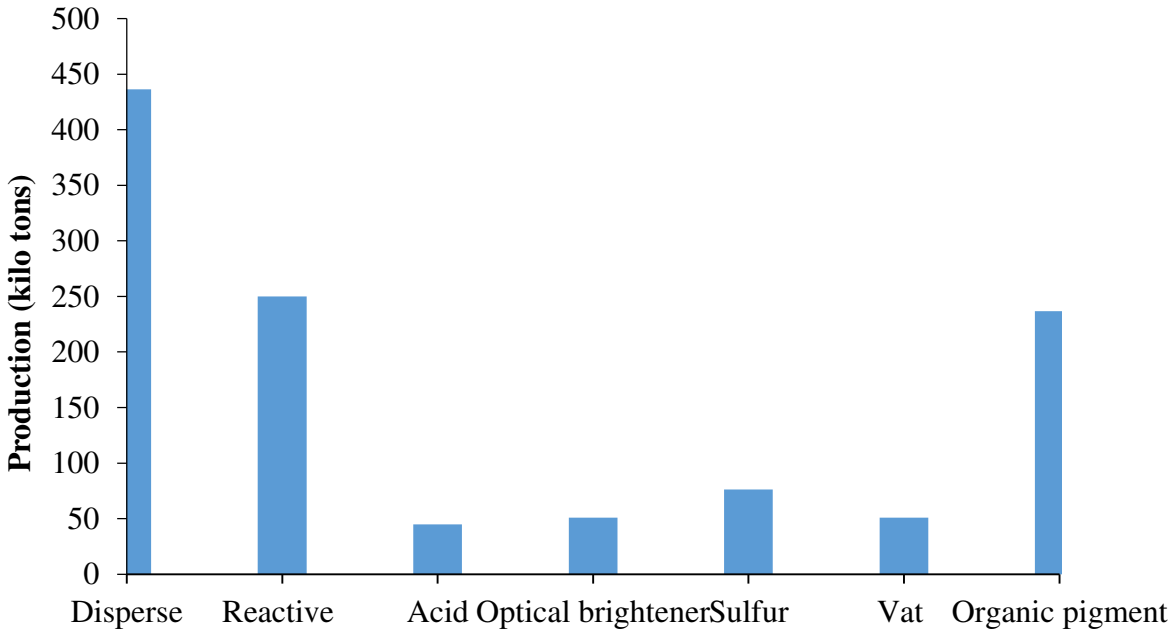

Fig. S1. Dyes and Pigments production data of China of 2016 [Statistical Yearbook of China, 2017].

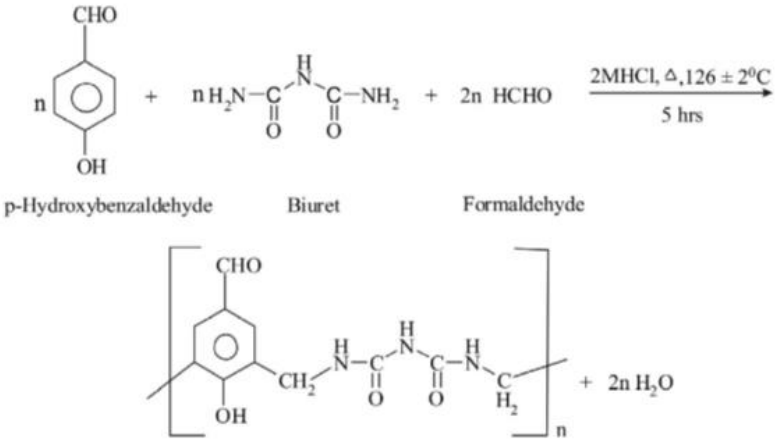

Fig. S2. Formation of terpolymer cation-exchange resin of p-hydroxybenzaldehyde, biuret and formaldehyde by condensation polymerization (Patle and Gurnule, 2016].

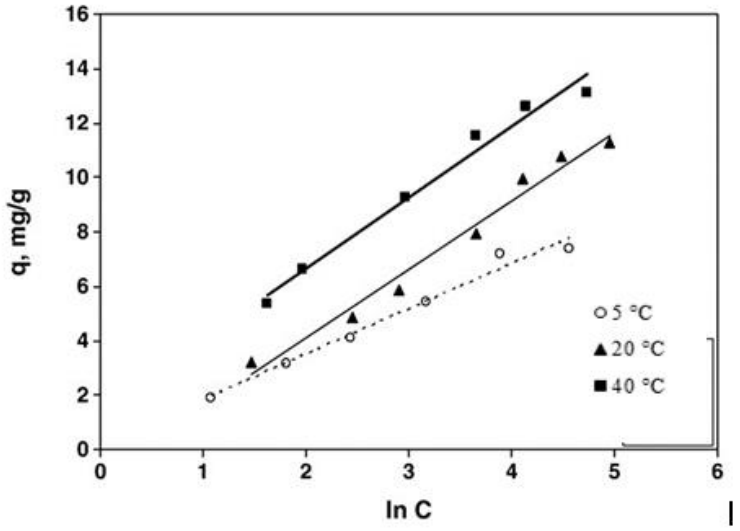

Fig. S3. The Temkin isotherm model of removal of C.I. Reactive Red 120 by lignin adsorbent [Suteu et al., 2010].

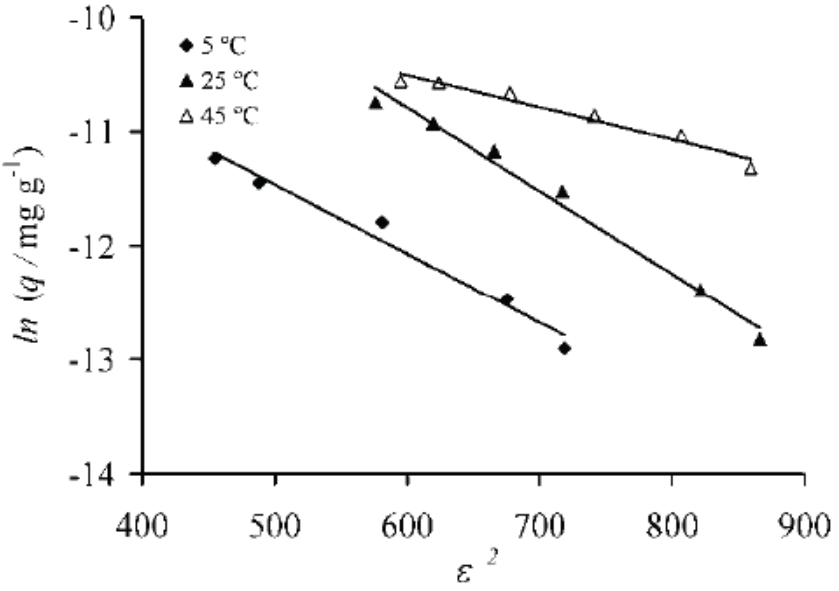

Fig. S4. The Dubinin–Radushkevich isotherm model of removal of C.I. Reactive Orange 16 by waste sunflower seed shells [Suteu et al., 2011].

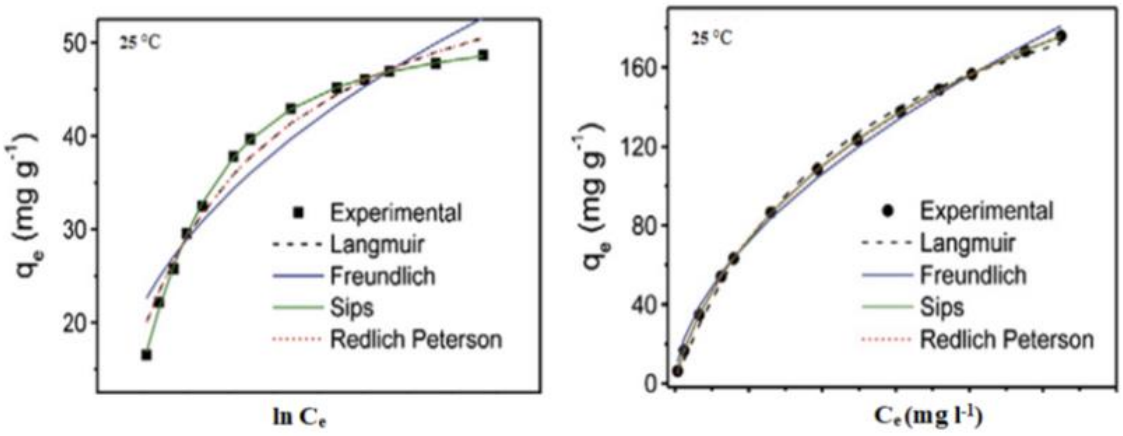

Fig. S5. The Sips and Redlich-Peterson isotherm models of removal of C.I. Reactive Black 5 by Brazilian pine fruit shell (left) and activated carbon made from it at 30 °C [Pinto et al., 2010].

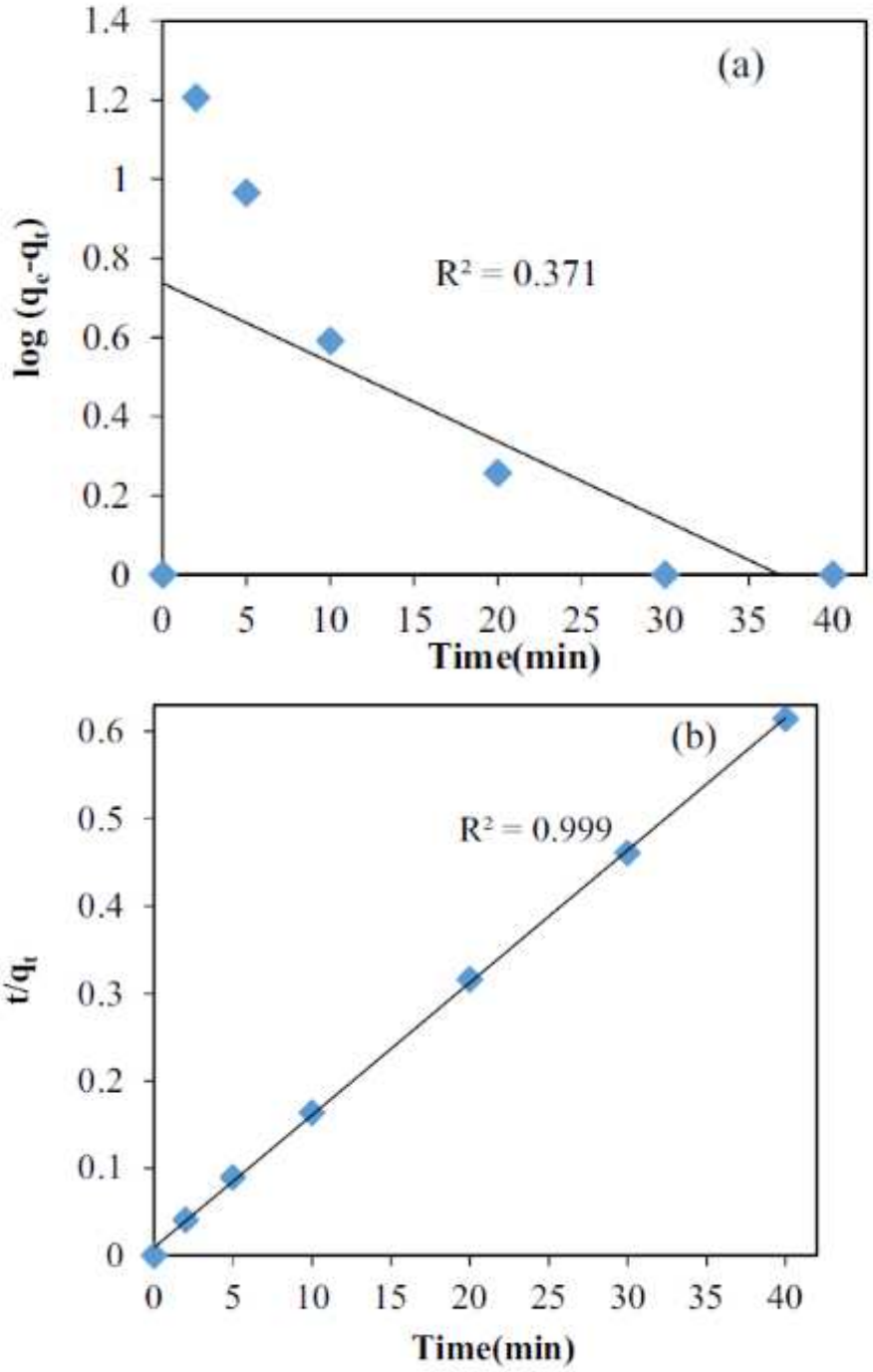

Fig. S6. Pseudo-first-order (a) and pseudo-second-order (b) reaction rate of adsorption of C.I. Reactive Blue 19 onto L-arginine-functionalised Fe_3O_4 nanoparticles [Dalvand et al., 2016].

Table S1

Reactive dye binding performance of various unmodified and modified carbonaceous and clay-like adsorbents

Adsorbents	Dye type	Treatment methods	Operating conditions						Absorption capacity ($mg\ g^{-1}$)	Ref.
			Temperature (°C)	pH of maximum adsorption	Dosage of sorbent ($g\ L^{-1}$)	Agitation speed (rpm)	Dye conc. ($mg\ L^{-1}$)	Contact time (min)		
Nanohydroxyapatite	C.I. Reactive Blue 19	Batch	20	3	2	200	65	180	31.06	[Kyzas et al., 2013]
Non-calcined Mg/Al LDH	C.I. Reactive Blue 4	Batch	22±1	2	0.75	n/a	n/a	140	328.9	[Aguiar et al., 2013]
Calcined Mg/Al LDH	C.I. Reactive Red 195	Batch	25±1	6	1	n/a	1817.6	1440	134.37	[Asouhidou et al., 2012]
Calcined Mg/Al LDH	C.I. Reactive Orange 16	Batch	25	5.6–6.6	0.2	100	50-100	1440	268.14	[Sumari et al., 2016]
	C.I. Reactive Red 120								256.07	
Bentonite	C.I. Reactive Black 5	Batch	30	10	5	100–240	50	60	22.71	[Amin et al., 2015]
Seawater-neutralised red mud	C.I. Reactive Blue 19	Batch	25	4	4	250	50–3000	60	255.6	[de Souza et al., 2013]
Seawater-neutralised red mud calcined at 400 °C									210.3	
Seawater-neutralised red mud calcined at 500 °C									284.4	
$MgCl_2$-modifed red mud	C.I. Reactive Blue 19	Batch		7	5–25	150	100		27.40	[Wang et al., 2009]
Thermally treated red mud	C.I. Reactive Blue 19	Batch	30	2	4	250	5000	180	178.4	[de Jesus et al., 2015]
Laccase-modified fumed silica	C.I. Reactive Black 5	Batch	30	9	1	n/a	0	60	322.58	[Kalkan et al., 2014]
Nano-alumina	C.I. Reactive Red 120	Batch	n/a	3	0.8	150	100	150	36.6	[Nadafi et al., 2014]
ZnO nanoparticles	C.I. Reactive Black 8	Batch	25±1	8	8	150	75	120	27.6	[Khoshhsab et al., 2015]
MgO nanoparticles	C.I. Levafix Fast Red CA	Batch	25	6	0.5	200	0.05	45	92.16	[Venkatesha et al., 2012]
Raw Fouchana clay	C.I. Reactive Red 120	Batch	19	6.3	30	450	30		9.3	[Errais et al., 2012]
Raw caolinite clay									9.8	
$Mg(OH)_2$-coated bentonite	C.I. Reactive Blue 19	Batch	25±1	6.5	2	200	120	300	47.21	[Chinoune et al., 2016]
Silylated palygorskite	C.I. Reactive Red 195	Batch	20	2	1-8	170	120–600	35	34.23	[Xue et al., 2010]
	C.I. Reactive Black 5								38.60	
	C.I. Reactive Blue 171								60.13	
Synthetic talc	Procion Brilliant red H-EXL	Batch	25±1	3.1	20	150	200	960	12.92	[Rahman et al., 2013]
Kaolin									4.51	

Table S2

Reactive dye removal performance of Removal of colour by microbial biomass

Ion-exchange resins	Dye type	Treatment methods	Operating conditions						Dye binding capacity (mg g^{-1})	Ref.
			Temperature of treatment (°C)	pH of maximum adsorption	Dosage of sorbent (g L^{-1})	Agitation speed (rpm)	Dye conc. (mg L^{-1})	Contact time (min)		
Bacterial biomasses										
Raw *E. coli* Esterified E. coli	C.I. Reactive Yellow 2	Batch	25	1	2.5	160	500	1440	196.89 335.17	[Kim et al., 2016]
Nostoc linckia	C.I. Reactive Red 198	Batch	25 35	2	1	120	300	120	273.8 422.5	[Mona et al., 2011]
Lemna gibba	C.I. Reactive Green 12	Batch	20	1	4	200	50	120	6.13	[Guendouz et al., 2016]
Corynebacterium glutamicum	C.I. Reactive Black 5	Batch	20 30 40	3	10	160	500	1440	169.5 175 185	[Won and Yun, 2008]
Corynebacterium glutamicum	C.I. Reactive Yellow 2	Batch	25±2	1	10	160	500	1440	178.5	[Vijayaraghavan, 2007]
Corynebacterium glutamicum	C.I. Reactive Black 5	Batch	35	1	2.5	160	500	720	195	[Won et al., 2006]
Mixture of Alcaligenes faecalis and *Commomonas acidovorans*	C.I. Reactive Black 5	Up-flow anaerobic filter	20	7	n/a	Flow rate = 100 ml h^{-1}	500	2880	95%	[Oxspring et al., 1996]
Paenibacillus azoreducens sp. nov.	C.I. Reactive Black 5	Batch	37	7	100 ml/l	50	100	1440	98.00 %	[Meehan et al., 2001]
Pseudomonas luteola free cells	C.I. Reactive Red 22	Batch	45	9.0	0.66	100	200	1440	32.3	[Chang et al., 2001]
Pseudomonas luteola	C.I. Reactive Red 22	Batch	28	n/a	1.0	450	200	60	113.7	[Chang et al., 2000]
Desulfovibrio desulfuricans	C.I. Reactive	Batch	35	7.0	0.3	n/a	100	2880	152.0	[Kim et al., 2007]
Aeromonas sp.	C.I. Reactive Black 5 C.I. Reactive Red 22 C.I. Reactive Violet 2	Batch	28	3	n/a	n/a	200	60	125 116.5 114.5	[Hu, 1996]
Lysinibacillus sp. Attached electrospun polysulphone mat	Reactive Blue 221 Reactive Black 5	Batch	23	6	0.2	100	10	14-day	15 36.5	[San Keskin et al., 2015]
Fungal biomasses										
Dead wood-rotting fungus (*Trametes versicolor*)	C.I. Reactive Blue 4	Batch	27±2	2	20	150	50	90	51.60	[Binupriya et al., 2007]
Rhizopus arrhizus	C.I. Reactive Black 5	Batch	35	2	1	150	800	1440	501	[Aksu and Tezer, 2000]
Rhizopus arrhizus	C.I. Reactive Blue 21	Batch	45	2	0.5	150	812.6	1440	773	[Aksu and Cagatay, 2006]
Aspergillus parasiticus	C.I. Reactive Red 198	Batch	20	2	2	200	300	60	101.37	[Akar et al., 2009]
Thamnidium elegans	C.I. Reactive Yellow 2	Batch	n/a	2	1.6	n/a	100	660	288.08	[Akar et al., 2017]
Thamnidium elegans	C.I. Reactive Yellow 2	Column	n/a	2	Flow rate = 2 ml min^{-1}		100	60	73.29	[Akar et al., 2017]
Fungal strain VITAF-1	C.I. Reactive Green 19	Batch	30	3	0.74	120	1000	2880	330.74	[Sinha and Osborne, 2016]
Rhizopus nigricans	C.I. Reactive Black 8	Batch	30	6	10	120	50	25	122	[Kumari and Abraham, 2007]
	C.I. Reactive Blue 3								123	
	C.I. Reactive Blue 38								161	
	C.I. Reactive Green 19								204	
Penicillium ochrochloron	C.I. Reactive Blue 13	Batch	n/a	2	2	150	0.05	120	55	[Aytar et al., 2016]

Penicillium restrictum	C.I. Reactive Black 5	Batch	35 20 50	1	0.4	200	200	75	142.04 98.33 112.50	[Iscen et al., 2007]
Rhizopus oryzae *Aspergillus versicolor* *Aspergillus niger* *Termitomyces clypeatus*	C.I. Reactive Blue 4	Batch	30	3	2	120	100	1440	49.25 26.7 25.08 24.28	[Bagchi and Ray, 2015]
Symphoricarpus albus	C.I. Reactive Red 45	Batch	25	2	8	200	100	60	22.48	[Kara et al., 2012]
Fungal biomass of mixed *Aspergillus versicolor* and *Rhizopus arrhizus* with dodecyltrimethylammonium bromide	C.I. Reactive Blue 19	Batch	n/a	6	n/a	n/a	100	6-day	100	[Gül and Dönmez, 2013]
Fungal biomass of mixed *Aspergillus versicolor* and *Rhizopus arrhizus*	C.I. Reactive Blue 19	Batch	n/a	6		n/a	100	6-day	86.5	[Gül and Dönmez, 2013]
Aspergillus fumigatus	C.I. Reactive Violet 5	Batch	30±2	3	n/a	100	100	7-day	98%	[Dharajiya et al., 2016]
Phanerochaete chrysosporium	C.I. Reactive Yellow 84								95%	
Aspergillus fumigatus	C.I. Reactive Violet 5			5					47.06	
Phanerochaete chrysosporium	C.I. Reactive Yellow 84								64.6	
Mixed cultures isolated from textile effluent under anaerobic conditions	C.I. Reactive Black 5	Batch	35	8	n/a	n/a	100	2880	100%	[Çetin and Dönmez, 2006]
	C.I. Reactive Red 21			7				1800	100%	
Aspergillus fumigatus isolated from textile effluent with 10 g/l sucrose	C.I. Reactive Blue 268	Batch	27	6	n/a	n/a	100	6-day	100%	[Karim et al., 2017]
Heat treated dead Aspergillus fumigatus biomass isolated from textile effluent					10				65.00%	
Microalgae										
Spirulina platensis	Reactive Red 120	Batch	25	2	2.5	n/a	1200	150	482.2	[Cardoso et al., 2012]
Enteromorpha prolifera	Reactive blue 171	Batch							71.94	[Sun et al., 2013]
	Reactive blue 4								131.93	
Chlorella vulgaris	C.I. Reactive Black 5	Batch	35	2	1	150	789.2	1440	555.60	[Bras et al., 2001]
	Remazol Red RR		25				198		196.1	
	C.I. Reactive Orange 107		25				198		71.9	